

Heartcare Suite: A Unified Multimodal ECG Suite for Dual Signal-Image Modeling and Understanding

Yihan Xie^{1,*}, Sijing Li^{1,*}, Zhuonan Wang^{1,*}, Tianwei Lin^{1,*}, Chenglin Yang¹, Yu Zhong¹, Wenjie Yan¹, Wenqiao Zhang¹, Xiaogang Guo¹, Jun Xiao¹, Yueting Zhuang¹, Beng Chin Ooi²

¹Zhejiang University, ²National University of Singapore

Abstract

Although electrocardiograms (ECG) play a dominant role in cardiovascular diagnosis and treatment, their intrinsic data forms and representational patterns pose significant challenges for medical multimodal large language models (Med-MLLMs) in achieving cross-modal semantic alignment. To address this gap, we propose **Heartcare Suite**, a unified ECG suite designed for dual signal-image modeling and understanding. (i) **Heartcare-400K**: We build a fine-grained ECG instruction dataset on top of our data pipeline engine—**HeartAgent**—by integrating 12,170 high quality clinical ECG reports from top hospitals with open-source data; (ii) **Heartcare-Bench**: a systematic benchmark assessing performance of models in multi-perspective ECG understanding and cross-modal generalization, providing guidance for optimizing ECG comprehension models; (iii) **HeartcareGPT**: built upon a structure-aware discrete tokenizer **Beat**, we propose the **DSPA (Dual Stream Projection Alignment)** paradigm—a dual encoder projection alignment mechanism enabling joint optimizing and modeling native ECG signal-image within a shared feature space. **Heartcare** achieves consistent improvements across diverse ECG understanding tasks, validating both the effectiveness of the unified modeling paradigm and the necessity of a high-quality data pipeline, and establishing a methodological foundation for extending Med-MLLMs toward physiological signal domains. Our project is available at <https://github.com/DCDmllm/Heartcare-Suite>.

1. Introduction

Multimodal large language models (MLLMs) [1, 3, 5, 10, 19, 24, 30, 33, 39, 46, 47] demonstrate strong performance in general-purpose scenarios by jointly modeling multiple modalities such as text, images, and video. Motivated by their success in open-domain scenarios, researchers have ex-

tended the MLLM paradigm to the medical domain, giving rise to medical multimodal large language models (Med-MLLMs), including LLaVA-Med [18], HuatuoGPT-Vision [9], HealthGPT [23], and Lingshu [44]. These models show potential for medical diagnosis and reasoning, driving progress in intelligent healthcare applications.

In fact, existing Med-MLLMs are constrained by vision-centric paradigms that focus on imaging data[27, 52], yet medical applications frequently require integration of non-imaging modalities and domain-specific knowledge[38]. ECG illustrates this limitation, as it encodes critical diagnostic information in a dual signal-image form, tightly combining temporal and morphological features[4, 43]. Consequently, ECG not only delineates the failure boundary of existing approaches but also highlights the fundamental rationale for developing dedicated Med-MLLMs: *the structural characteristics of medical modalities must serve as the foundation of model design, rather than an afterthought for adaptation.*

Intelligent ECG interpretation relies on symbolic semantics to integrate patient history, ECG data, and clinical reports into interpretable reasoning chains. This paradigm, naturally suited to MLLMs, still faces fundamental challenges:

Data Misalignment. Mainstream ECG datasets such as PTB-XL [42] are designed for rhythm and disease classification, with annotations at the global level and lacking step-wise supervision. As a result, these datasets mainly enable direct mapping from ECG signals to labels, making it difficult to support interpretable reasoning or cross-modal information integration, and thus limiting the shift from simple classification to deeper understanding and reasoning.

Evaluation Deficiency. Existing medical benchmarks primarily emphasize classification accuracy and tend to overlook the assessment of comprehensive reasoning processes[26, 40]. For instance, they rarely evaluate models’ capabilities in clinical reasoning or pathology QA for ECG tasks. Therefore, it is essential to develop multidimen-

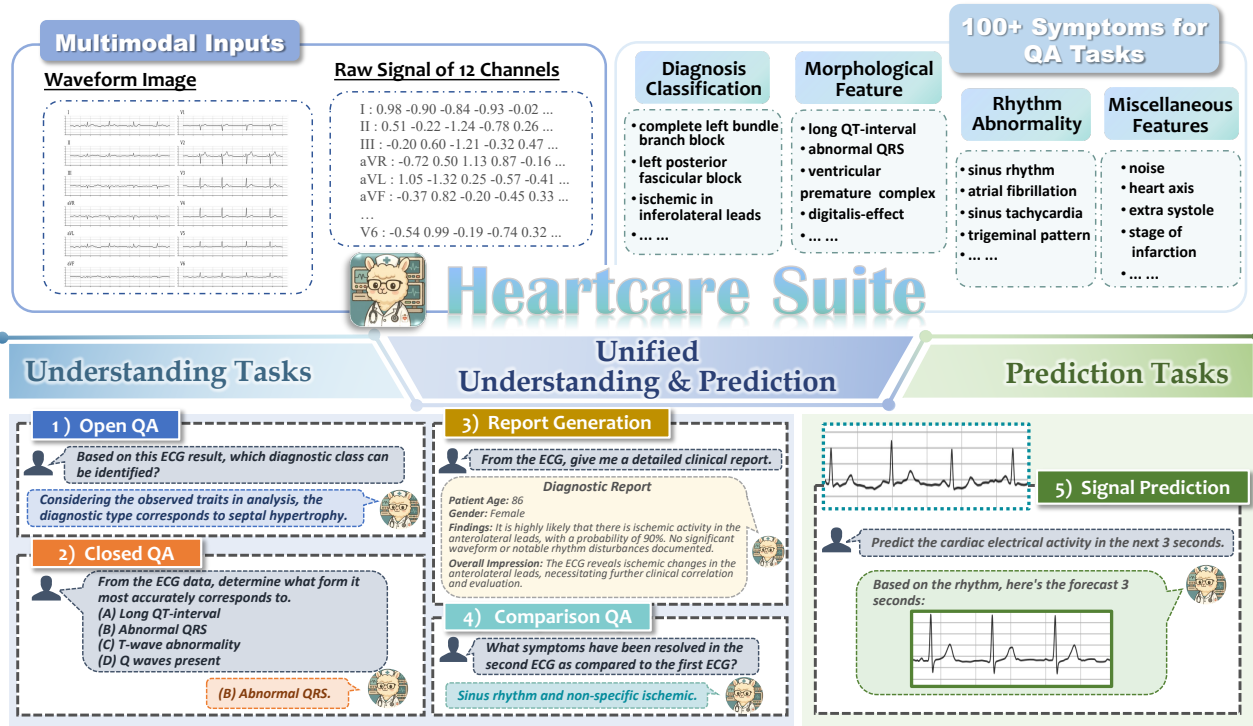


Figure 1. The proposed **Heartcare-400K** dataset. Heartcare-400K aggregates real-world ECG data, supporting Closed-QA, Open-QA, Report Generation and Signal Prediction.

sional assessment frameworks that include reliability and scenario-based metrics for evaluating the clinical utility of ECG-specific Med-MLLMs.

Dual Signal-Image Fusion Incapacity. The dual nature of ECG data—comprising both raw temporal signals and waveform images—poses unique modeling challenges[34, 37]. While signals capture dynamic cardiac activity and images reflect spatial morphology, both are essential for diagnosis. Most vision-focused MLLMs, however, process only ECG images [2, 28], neglecting key temporal features in the signal, such as intervals, calibration, inter-lead phase, and beat-to-beat changes. Moreover, multi-lead synchronous acquisition results in a tightly coupled, heterogeneous structure across temporal and spatial domains[21]. Addressing this dual complexity requires Med-MLLMs capable of consistent multimodal modeling and alignment.

We propose **Heartcare Suite**—a systematic and innovative framework for ECG, dedicated to establishing a unified and extensible ecosystem for ECG-specific Med-MLLMs:

(i) Dataset. We construct **Heartcare-400K**, a large-scale, fine-grained, multi-task multimodal ECG instruction dataset. It combines two sources: the public PTB-XL dataset [42] with 21,799 12-lead ECG signals annotated with 179 SCP-ECG classes, and 12,170 ECG images with structured reports from top hospitals, including scanned traces, clinical conclusions, and de-identified metadata—substantially enriching modality and label diversity. To transform heterogeneous

ECG data into structured annotations, we develop **HeartAgent**, a multimodal engine with a bottom-up pipeline that ensures annotation consistency and generates high-quality instruction-style VQA pairs.

(ii) Benchmark. We propose **Heartcare-Bench**, the first fine-grained, multidimensional evaluation framework for ECG diagnostic intelligence, designed to assess a spectrum of model capabilities ranging from feature recognition to reasoning. Built upon Heartcare-400K, Heartcare-Bench systematically covers five major task types—closed-ended QA, open-ended QA, comparative QA, report generation, and signal prediction—spanning key diagnostic dimensions such as rhythm, waveform, and morphology. It comprises three complementary modality subsets: *Signal (S)*, *Image (I)*, and *Cross-Modal (C)*, enabling unified evaluation from single-modality reasoning to multi-ECG semantic alignment. With a hierarchical, multi-metric scoring system, Heartcare-Bench integrates knowledge reasoning and cross-modal understanding within a unified evaluation coordinate.

(iii) Model. The dual-form characteristics of ECG introduce unique structural complexity in modeling. We propose **HeartcareGPT**, aiming to build ECG-specific Med-MLLMs. We design **Bidirectional ECG Abstract Tokenization (Beat)**, a structure-aware discrete encoding mechanism centered on vector quantization [11, 41, 50], which maps high-frequency continuous signals into token sequences. The design comprises three components: (i) *Dual-level Vector*

Quantization (DVQ), which refines rhythm and inter-lead phase dependencies captured by the codebook to achieve high-fidelity compression; (ii) *Query-guided Bidirectional Diffusion (QBD)*, which jointly models past and future contexts within the latent token space to support both signal reconstruction and prediction; and (iii) *Joint Supervision Strategy*, which jointly optimizes reconstruction and prediction to maximize clinical semantic fidelity during encoding. Furthermore, we propose **Dual Stream Projection Alignment (DSPA)**, which employs dual experts to separately process ECG inputs. Through distinct preprocessing strategies and modality-specific encoders, ECG representations are transformed into embeddings compatible with Med-MLLMs. All modality embeddings are projected into a shared language space and concatenated into a unified sequence, enabling cross-modal joint reasoning for ECG under a unified autoregressive paradigm.

Experimental results demonstrate the powerful paradigm of Heartcare Suite. The main contributions of this work are as follows:

- **High-quality ECG Instruction Dataset.** Heartcare-400K serves as the first comprehensive ECG instruction dataset, which significantly enhances Med-MLLM performance across ECG-related tasks.

- **Multidimensional ECG Benchmark.** We propose Heartcare-Bench, a evaluation framework that assesses clinical performance of ECG tasks for Med-MLLMs.

- **Fine-grained ECG Understanding Paradigm.** We develop HeartcareGPT, the first model supporting pathology-level ECG understanding with SoTA results.

2. Related Work

Multimodal Representation Learning for ECG. Recent advances in multimodal ECG representation learning follow three main directions. First, signal-semantic alignment. ECG-SL [48] and MERL [17] align heartbeats and clinical reports via self-supervision and knowledge prompting, while HeartLang[17] decomposes waveforms into semantic tokens for fine grained cardiac analysis. Second, cross-lead fusion. ECG-DAN[8] adopts a dual attention network to balance global cross lead interactions with local temporal dynamics, and ESI[49] adds a signal text contrastive learning to strengthen robustness under limited labels. Third, LLM-driven pretraining. ECG-LM[45] maps ECG embeddings into a pretrained language space, and SuPreME[6] structures domain knowledge from clinical reports for pretraining. However, existing approaches typically address isolated aspects such as reconstruction quality, lead interaction, or semantic alignment, without forming a unified end-to-end multimodal ECG modeling framework.

Medical Multimodal Large Language Models. Med-MLLMs have shown strong capabilities in medical understanding and diagnostic support [9, 16, 32, 44]. Med-

Flamingo [26] and LLaVA-Med [18] are representative early medical multimodal models, focusing on image-text alignment and visual question answering. MedVLM [32] employs multi-stage pretraining and attains state-of-the-art performance in radiology report generation and organ localization. HealthGPT [23] unifies image understanding and generation within one framework. Domain-specific variants—LLaVA-Rad [7], EyecareGPT [20], and SkinGPT-4 [53]—enable structured reporting and multimodal reasoning across radiology, ophthalmology, and dermatology. However, the dual-form characteristics of ECG presents significant challenges to vision-centric models, and an effective ECG-specific Med-MLLM framework remains absent to date.

3. Heartcare Suite: Heartcare-400K

3.1. Data Collection and Organization

Existing ECG datasets suffer from limited modalities, coarse annotations, insufficient scale, and substantial heterogeneity in signal sampling, lead configuration, and preprocessing, all of which hinder the development of Med-MLLMs for intelligent ECG diagnosis. To address these gaps, we introduce **Heartcare-400K**, a large-scale multimodal ECG VQA dataset with two complementary modalities: (i) **structured digital signals** and (ii) **unstructured ECG report images**. We normalize them by rendering all signals into a unified ECG visual format consistent with clinical layout. These visualized signals, together with native report images, enrich modality diversity and support comprehensive ECG understanding.

To construct Heartcare-400K, we collaborated with several major public hospitals to collect 12,170 standardized PDF-format clinical ECG reports. These reports include patient demographics, physiological parameters, physician diagnoses, and about 5 seconds of 12-lead waveform images. In addition, we systematically integrated multiple publicly available digital signal ECG datasets, with PTB-XL as the primary source. PTB-XL is one of the largest open ECG repositories, containing 21,799 12-lead records sampled at 500 Hz over 10 seconds, with standardized diagnostic labels and detailed patient metadata (such as sex, age and weight).

Raw ECG data typically contain only brief diagnostic text and lack the instruction-style supervision and semantic diversity needed for VLM fine-tuning. To address this, we developed a multimodal data engine for automated extraction, cleaning, standardization, and expert review, and further augmented the dataset with QA pairs from the publicly available ECG-QA [29], which supports both single-modality queries and cross-modality reasoning tasks.

Ultimately, Heartcare-400K is organized into four types of VQA tasks: (i) closed-QA (single-ECG multiple-choice question), (ii) open-QA (single-ECG short-form question), (iii) comparison-QA (multi-ECG multiple-choice question), report generation (long-form answers), and (iv) signal pre-

diction (ECG generation). These tasks equip models with fine-grained ECG comprehension and clinical reasoning capabilities, making Heartcare-400K a foundational resource for developing practical and generalizable intelligent ECG diagnosis systems.

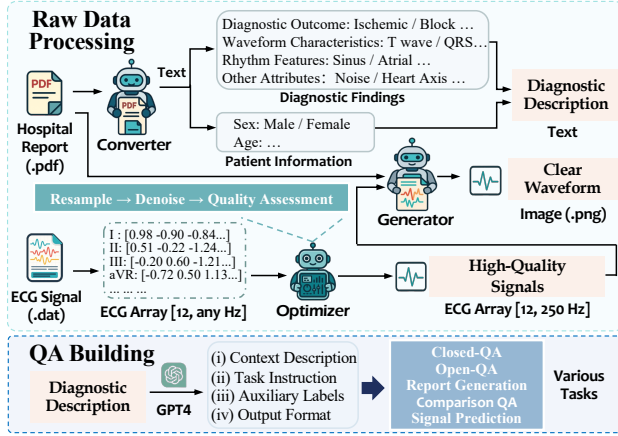


Figure 2. Framework of multimodal data engine for QA generation.

3.2. Multimodal Data Engine

To efficiently construct Heartcare-400K, we design **HeartAgent** (as shown in Figure 2), an automated multimodal data engine with two key stages: *raw data processing* and *data building*. Details of each module are provided in the Appendix A.

Raw Data Processing. This stage integrates three core components to transform heterogeneous ECG sources into standardized inputs: (i) **Multimodal Feature Converter**: Extracts patient information and clinical descriptions from hospital PDFs, maps diagnostic text to structured labels, and prepares both text and image data for subsequent processing. (ii) **Noise Filtering and Quality Optimizer**: Unifies signal formats and applies denoising, resampling, and quality assessment to produce high-quality, standardized ECG signals. (iii) **Diversified Image Generator**: Renders clean waveform images from processed digital signals and generates de-identified tracings from hospital reports, ensuring multi-modal data alignment.

Data Building. The final stage is handled by the **Multi-task QA Builder**, which constructs instruction-style QA samples using GPT-4. Each sample contains structured context, clear task instructions, auxiliary labels, and standardized answers, supporting four diverse ECG understanding tasks and a signal prediction task critical for comprehensive model training.

These components collectively ensure Heartcare-400K achieves high-quality, diverse, and task-relevant multimodal annotations.

4. Heartcare Suite: Heartcare-Bench

To systematically evaluate the capabilities of Med-MLLMs across unified ECG understanding and prediction tasks, we propose Heartcare-Bench—a multidimensional benchmark encompassing five major task types: closed-QA, open-QA, comparison-QA, report generation, and signal prediction. Heartcare-Bench is structured into three complementary subsets based on input modality: (i) signal-based (**Heartcare-Bench^S**), (ii) image-based (**Heartcare-Bench^I**), and (iii) cross-modal comparison (**Heartcare-Bench^C**). In addition, Heartcare-Bench employs strict patient-level data partitioning with thorough cross-split duplicate inspection; full details are provided in B.4.

Heartcare-Bench^{SI}: Single-Modality Subsets. The signal and image subsets share a unified framework to evaluate four core clinical dimensions: *Diagnosis*, *Waveform analysis*, *Rhythm interpretation* and *Miscellaneous Features*. To broaden task diversity and clinical relevance, we further integrate QA pairs from ECG-QA dataset [29], primarily those derived from PTB-XL, enriching closed- and open-QA settings and enabling categorization by these four dimensions. The *Misc.* category further assesses ECG attributes such as noise, infarction stage, ectopic beats, and cardiac axis. In addition to QA tasks, the single-modality subsets also include report generation and signal prediction tasks. Detailed formats and examples are provided in Appendix B.4.

Heartcare-Bench^C: Cross-Modality Comparison Subset. Beyond single-modality tasks, this subset evaluates a model’s ability to reason over multiple ECGs through comparison QA tasks adapted from ECG-QA [29]. It is centered around three modality comparison dimensions: (i) *signal-signal (S-S)*, (ii) *image-image (I-I)*, and (iii) *signal-image (S-I)*. Each configuration is further categorized into two clinically relevant subtypes: consecutive (ECGs from the same patient, assessing temporal consistency) and irrelevant (ECGs from different patients, evaluating differential diagnostic reasoning).

Overall, **Heartcare-Bench** adopts a multidimensional evaluation protocol covering semantic consistency, linguistic fluency, clinical accuracy, and waveform prediction quality. Full scoring rules and evaluation details are provided in Appendix B.4.

5. Methodology

5.1. Bidirectional ECG Abstract Tokenization

Forward Diffusion Process. Given an acquired ECG signal, we denoise and resample it to obtain a representative segment $\mathbf{S} \in \mathbb{R}^{T \times C}$ (sequence length T , C leads). We then partition \mathbf{S} into contiguous, non-overlapping temporal patches and map them with a projection layer Ψ to yield the

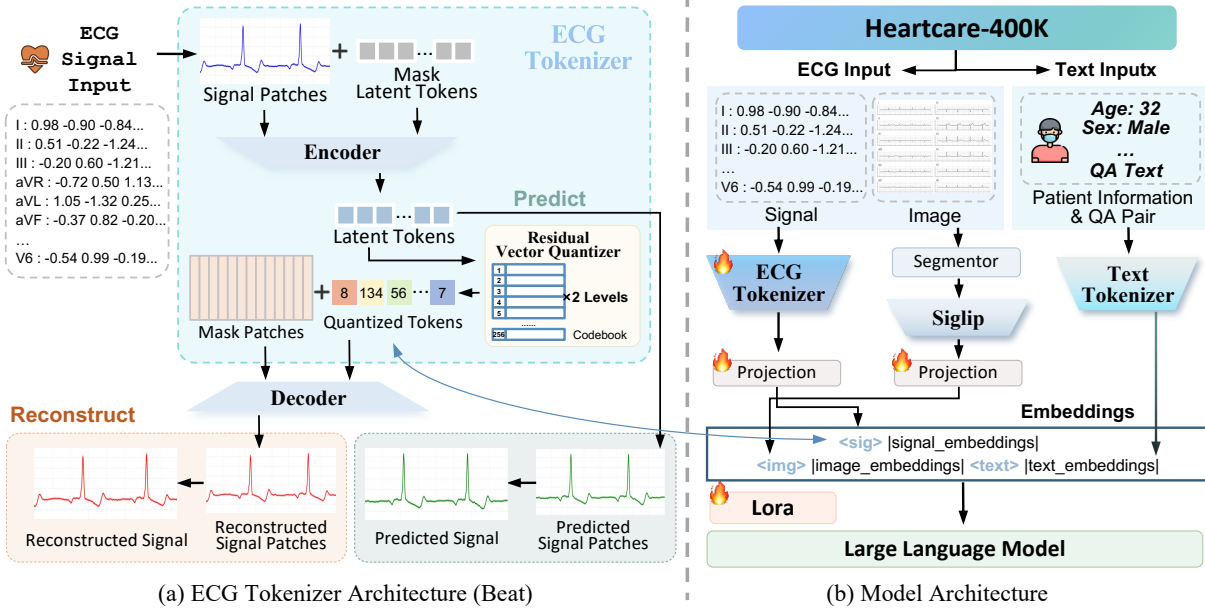


Figure 3. Architecture of HeartcareGPT. The dual-form ECG inputs are routed and encoded with modality-specific expert projections aligned to the LLM backbone. The unified autoregressive architecture efficiently supports interleaved and joint modeling of ECG multimodal inputs.

corresponding patch embeddings:

$$\mathbf{e} = \Psi(\text{Patchify}_f(\mathbf{S}) \mid \theta_\Psi) \in \mathbb{R}^{t \times c}, t = \frac{T}{f}, c = Cf, \quad (1)$$

where f is the patch frame size, t the number of patches, and θ_Ψ the projection parameters. To inject high-level semantic control, we append m learnable queries $\mathbf{q} \in \mathbb{R}^{m \times c}$ to the patch embeddings \mathbf{e} , forming the model input $\mathcal{H}_{\text{in}} = [\mathbf{e} \parallel \mathbf{q}]$. A Transformer encoder then performs forward diffusion, yielding compressed contextual representations:

$$\mathcal{H}_{\text{latent}}^q = (\text{TransformerEnc}(\mathcal{H}_{\text{in}}))_{[t:t+m]} \in \mathbb{R}^{m \times c}. \quad (2)$$

Dual-level Vector Quantization. To compress ECG signals while preserving rhythmic structure and salient pathological cues, we adopt dual-level VQ with a core codebook \mathcal{C}_1 and a residual codebook \mathcal{C}_2 . For each query vector $\mathbf{h}_q^i = (\mathcal{H}_{\text{latent}}^q)_{[i,:]} \in \mathbb{R}^c$, we first apply core quantization:

$$\hat{\mathbf{h}}_{(q,1)}^i = \text{Quant}_{\mathcal{C}_1}(\mathbf{h}_q^i) = \arg \min_{\mathbf{c} \in \mathcal{C}_1} \|\mathbf{h}_q^i - \mathbf{c}\|_2. \quad (3)$$

The residual is subsequently quantized by the codebook \mathcal{C}_2 :

$$\hat{\mathbf{h}}_{(q,2)}^i = \text{Quant}_{\mathcal{C}_2}(\mathbf{h}_q^i - \hat{\mathbf{h}}_{(q,1)}^i) = \arg \min_{\mathbf{c} \in \mathcal{C}_2} \|\mathbf{h}_q^i - \hat{\mathbf{h}}_{(q,1)}^i - \mathbf{c}\|_2. \quad (4)$$

Finally, we quantize the forward-diffused representation to $\hat{\mathbf{h}}_{\text{latent}}^i = \hat{\mathbf{h}}_{(q,1)}^i + \hat{\mathbf{h}}_{(q,2)}^i$, yielding a high-fidelity mapping from continuous latents to a discrete code space and significantly improving reconstruction quality.

Query-guided Bidirectional Diffusion. Forward diffusion (Eq. 2) compresses the ECG into a dense discrete space

but offers no guarantees of completeness or invertibility. We therefore adopt an autoencoding view and introduce a reverse diffusion anchored at the quantized query $\mathcal{H}_{\text{latent}}^q$, casting compression and reconstruction as a joint constraint: the forward path enforces compact coding, the reverse path restores details, yielding a closed-loop, bidirectional token refinement between latent and signal spaces.

During reverse diffusion, the original input \mathbf{e} is mapped to its forward-diffusion slot $\mathcal{H}_{\text{origin}}^q$ and masked by \mathcal{M} to prevent leakage, so only the query vectors $\mathcal{H}_{\text{latent}}^q$ retain ECG signal information for reconstruction:

$$\mathcal{H}_{\text{out}}^{\text{recon}} = (\text{TransformerDec}(\mathcal{H}_{\text{latent}}^q; \mathcal{M}))_{[0:t]}. \quad (5)$$

Joint Supervision Strategy. To fully exploit the bidirectional diffusion capacity, Beat employs a multi-objective loss that jointly optimizes reconstruction and compression, integrating three objectives. The reconstruction and prediction losses are defined as:

$$\mathcal{L}_{\text{recon}} = \|\mathcal{H}_{\text{out}}^{\text{recon}} - \mathbf{e}\|_2, \quad \mathcal{L}_{\text{pred}} = \|\mathcal{H}_{\text{latent}}^q - \mathbf{e}_{\text{pred}}\|_2. \quad (6)$$

where \mathbf{e}_{pred} denotes the ECG segment used for prediction. The vector quantization loss is defined as:

$$\mathcal{L}_{\text{VQ}} = \sum_{i,j} \|\text{sg}[\mathbf{h}_i^i] - \hat{\mathbf{h}}_{(q,i)}^i\|_2^2 + \beta \|\mathbf{h}_j^i - \text{sg}[\hat{\mathbf{h}}_{(q,j)}^i]\|_2^2, \quad (7)$$

where $\text{sg}[\cdot]$ denotes the stop-gradient operation, and \mathbf{h}_j^i refers to the feature vector before quantization at the j -th level.

The overall training objective is given by $\mathcal{L}_{\text{total}} = \lambda_1 \mathcal{L}_{\text{recon}} + \lambda_2 \mathcal{L}_{\text{pred}} + \lambda_3 \mathcal{L}_{\text{VQ}}$.

Tokenization. During inference, we discard the decoder and prediction heads, retaining only the encoder and quantizer. Given an ECG segment \mathbf{S} of length T , Beat applies temporal normalization: if $T > t$, split into $\lceil T/t \rceil$ slices from right to left; if $T < t$, left-pad to t . For recordings with fewer than 12 leads, pad missing channels with zeros. Each segment is then encoded into discrete tokens:

$$\mathcal{S} = \text{Beat}(\mathbf{S}) = \{c_1^1, \dots, c_1^n \| c_2^1, \dots, c_2^n\}, c_i^j \in \{\mathcal{C}_1, \mathcal{C}_2\}. \quad (8)$$

These discrete tokens can be directly used as multimodal extensions of LLM vocabulary, enabling unified semantic modeling and cross-modal reasoning between ECG signals and texts.

For autoregressive forecasting, Beat predicts the next t' segment conditioned on the previous context $(T + t')$, iteratively generating arbitrary-length ECG sequences.

5.2. HeartcareGPT

We present **HeartcareGPT**, which maps ECG signals, ECG images, and text into a unified discrete space, enabling ECG reasoning with a single autoregressive architecture.

Unified ECG Tokens. Specifically, for a multi-lead ECG $S \in \mathbb{R}^{T \times C}$, Beat (Eq. 8) encodes it into a token sequence \mathcal{S} capturing elementary ECG morphology. For ECG images, we partition and rearrange them into 12 lead-wise maps to decouple lead semantics, then apply SigLip [51] to obtain visual tokens \mathcal{V} that embed per-lead waveform and spatial layout. Meanwhile, clinical notes, basic physiological data, and diagnostic instructions are tokenized by the LLM’s native tokenizer into textual features $\mathcal{F}_{\mathcal{T}}$, providing a semantic anchor for non-text modalities and enabling fine-grained alignment and joint modeling in the shared token space.

Dual Stream Projection Alignment. To avoid parameter interference among modalities in shallow layers, we adopt a decoupled design, mapping each modality feature into the model’s embedding space through dedicated expert projections Ψ_{sig} and Ψ_{img} :

$$\mathcal{F}_{\mathcal{S}} = \Psi_{\text{sig}}(\mathcal{S} | \theta_{\Psi_{\text{sig}}}), \quad \mathcal{F}_{\mathcal{V}} = \Psi_{\text{img}}(\mathcal{V} | \theta_{\Psi_{\text{img}}}), \quad (9)$$

so that they lie in the same representation space. Either projection layer is implemented as a lightweight MLP block. Subsequently, at the input side we directly concatenate $\mathcal{F}_{\mathcal{S}}$, $\mathcal{F}_{\mathcal{V}}$, and the textual features $\mathcal{F}_{\mathcal{T}}$ into a single long sequence:

$$\langle \text{BOS} \rangle \langle \text{sig} \rangle \{ \mathcal{F}_{\mathcal{S}} \} \langle \text{img} \rangle \{ \mathcal{F}_{\mathcal{V}} \} \langle \text{text} \rangle \{ \mathcal{F}_{\mathcal{T}} \} \langle \text{EOS} \rangle, \quad (10)$$

where $\langle \text{sig} \rangle$ and $\langle \text{img} \rangle$ are specially introduced conditional tokens that can be expanded as needed at the implementation level to accommodate multiple signal segments and multiple images. With this design, the routing and composition of

multimodal inputs no longer rely on additional architectural components, but are uniformly reduced to simple template filling of instruction prompts.

Training Strategy. To enable stable coexistence of tokens from heterogeneous modalities and distributions within the base model, HeartcareGPT adopts an overall training pipeline with clearly separated roles: **(i) Multimodal warm-up**, where we only train the signal and image projection layers using a captioning task to preliminarily align multimodal features with textual features; **(ii) Joint fine-tuning**, where, once all modalities have been embedded into a compatible space, we unfreeze the weights of the LLM and optimize it together with the modality projection layers in an end-to-end manner on instruction tasks.

Autoregressive Multimodal Generation. The unified training objective of the model is to generate the corresponding textual output $\mathcal{R} = [r_1, r_2, \dots, r_{N_r}]$ conditioned on the above multimodal input $\mathcal{U} = \{\mathcal{F}_{\mathcal{S}}, \mathcal{F}_{\mathcal{V}}, \mathcal{F}_{\mathcal{T}}\}$, by maximizing the following probability distribution:

$$P_{\theta}(\mathcal{R} | \mathcal{U}) = \prod_{j=1}^{N_r} P_{\theta}(r_j | \{\mathcal{U} \| r_{<j}\}). \quad (11)$$

Here, θ denotes the parameters of \mathcal{M}_{llm} . The above optimization equips the model with strong capabilities in ECG diagnosis and cross-modal knowledge complementation, yielding a general paradigm for ECG specific Med-MLLMs.

6. Experiments

6.1. Data and Experimental Setup

Data Details. We systematically evaluate our model with baseline models on the proposed Heartcare-Bench^S, Heartcare-Bench^I and Heartcare-Bench^C, providing a comprehensive assessment of generalization and diagnostic accuracy. For baseline models that cannot accept digital signal input directly, we convert signals into image form. More details are provided in Appendix B.3.

Model Details. HeartcareGPT employs SigLip [51] and the proposed Beat as dual-form feature encoders and adopts a three-stage training paradigm: (i) training Beat to extract high-fidelity ECG embeddings, (ii) warming up the visual and signal projectors to stabilize feature alignment, and (iii) performing joint instruction fine-tuning on Heartcare-400K for end-to-end modeling. Detailed hyperparameter settings and model configurations are provided in Appendix B.

Baseline. We conduct a zero-shot evaluation on 12 representative LLMs, including eight open-world LLMs (e.g., LLaVA-v1.5 [18], Qwen2.5-VL [5], InternVL2.5 [10], Yi-VL [47], MiniCPM-V2.6 [12], gemma-3 [39], Claude3.5 [1], GPT5 [31] and four Med-MLLMs (e.g., Lingshu-7B [44], LLaVA-Med [18], MedVLM-R1 [32], HealthGPT [23]). Signal prediction tasks are not included in the evaluation when

baseline models fail to respond to the signal prediction instructions correctly. More details refer in Appendix B.1.¹

6.2. Main Results

Closed-QA. As shown in Table 1, HeartcareGPT-7B achieves SoTA performance on closed QA with an average accuracy of 83.42%, while HeartcareGPT-3.8B achieves 83.33%, surpassing other models across all subtasks by a large margin. We attribute this to the ECG-aware tokenization and instruction tuning framework, which enables precise alignment between temporal signal patterns and clinically grounded language reasoning.

Open-QA. Table 2 reports the results on open-ended ECG QA, evaluated using BioBERTScore-F1 (*F1-Bio*) and *ROUGE-L*. Our HeartcareGPT series achieve the highest overall performance across four subtasks, demonstrating strong capability in generating clinically relevant, semantically consistent answers grounded in ECG signals.

Comparison-QA. The Comparison-QA task assesses cross-modal reasoning by requiring analysis and contrast of two ECG inputs—either signals, images, or signal-image pairs—in Heartcare-Bench^C. As shown in Table 3, HeartcareGPT excels in this challenging setting, with both the 3.8B and 7B models achieving state-of-the-art performance. This success underscores the effectiveness of our multimodal fusion design, which enables a unified and nuanced understanding across heterogeneous ECG representations.

Report Generation. Table 4 presents HeartcareGPT’s report generation results on Heartcare-Bench^S and Heartcare-Bench^I, evaluated by Score^{GPT}, F1-Rad, and ROUGE-L. HeartcareGPT achieves top scores on most metrics, outperforming all baseline models. While Qwen2.5-VL-7B scores higher on some metrics related to report structure and expression, HeartcareGPT excels in clinical content accuracy and reliability. Since GPT-based evaluation considers formatting and completeness, score differences often reflect output style rather than clinical accuracy. Full criteria and model comparisons are detailed in Table 9.

6.3. Ablation Study and Expert Evaluation

We conduct extensive ablation studies to analyze the contribution of each design component in HeartcareGPT. The complete results are presented in Appendix C.1.

The Three-Stage Training Pipeline. We further verify the necessity of each training stage in our three-phase optimization scheme. We experiment with models that omit (i) Step 1: beat-level training, (ii) Step 2: projector warming-up, and (iii) both steps simultaneously. Figure 4 show our results of ablation studies on the training pipeline. The performance significantly drops in all ablated variants, indicating that each

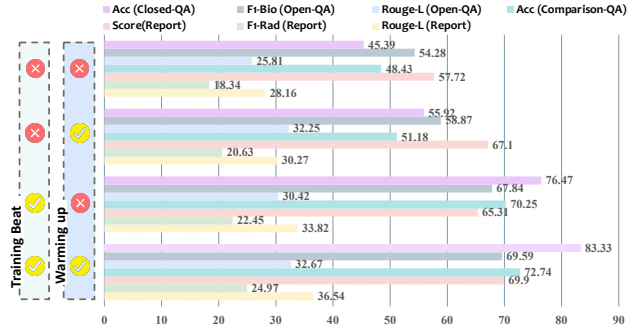


Figure 4. Results of ablation studies on training pipeline.

stage plays an indispensable role in stabilizing multimodal alignment and improving diagnostic accuracy.

Multimodal Integration. To assess multimodal fusion, we compare our tri-modal (signal-image-text) model against single-modality baselines (image-only and signal-only). We further examine ECG image segmentation by contrasting full-image and 12-lead sub-image strategies. As summarized in Figure 5 (a), multimodal fusion and sub-image segmentation yield clear performance gains, highlighting the value of integrating diverse ECG modalities for improved diagnostic understanding.

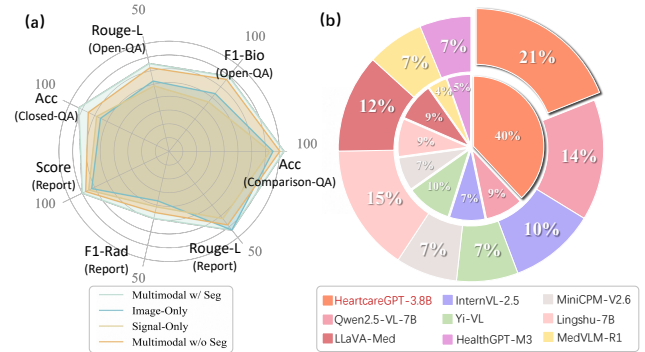


Figure 5. (a) Results of ablation studies on multimodal integration. (b) Expert Preference Distribution Across Models. Inner-ring results are based on Open-QA evaluations; outer-ring results are based on report generation evaluations.

Expert Evaluation. We conduct expert evaluation to assess clinical preference on Open-QA and report-generation tasks. Ten board-certified cardiologists reviewed 400 sampled cases with shuffled outputs from HeartcareGPT-3.8B and eight representative baselines, selecting responses best aligned with clinical reasoning and diagnostic conventions. As shown in Figure 5(b), HeartcareGPT achieves the highest first-choice selections—40% in Open-QA and 21% in report generation—substantially surpassing all baselines (7–15%). These results demonstrate clear clinical preference for HeartcareGPT, with expert scoring consistent with automated metrics, further supporting its clinical reliability.

¹Due to space constraints, some experimental results are included in the Appendix C.

Table 1. Performance comparison between HeartcareGPT and other baselines on *closed-QA* task from our proposed Heartcare-Bench^S and Heartcare-Bench^I. We use **bold** text to indicate the best results and underline to indicate the second-best results.

Model	Heartcare-Bench ^S				Heartcare-Bench ^I				Avg.
	Diagnosis	Waveform	Rhythm	Misc.	Diagnosis	Waveform	Rhythm	Misc.	
<i>Generalist Models</i>									
LLaVA-1.5-7B [24]	19.26	27.03	22.19	28.96	15.15	12.40	18.20	25.47	21.08
Qwen2.5-VL-7B [5]	28.29	35.36	31.70	35.31	35.84	31.06	22.35	41.41	32.67
InternVL-2.5-8B [10]	29.87	34.18	31.25	40.75	25.86	17.89	38.23	40.05	32.26
Yi-VL-6B [47]	49.19	38.90	31.06	39.65	59.55	44.46	17.06	39.85	39.97
MiniCPM-V2.6-8B [12]	32.37	31.34	23.40	32.23	23.71	33.59	10.05	30.63	27.17
Gemma-3-4B [39]	23.84	24.36	18.30	21.47	38.73	38.09	20.63	19.32	25.59
Claude-3.5 [1]	37.37	20.73	15.96	35.16	30.58	37.76	37.83	34.45	31.23
GPT5 [31]	29.87	15.23	19.57	25.23	41.42	34.14	33.73	26.23	28.30
<i>Medical Models</i>									
Lingshu-7B [44]	29.56	33.44	40.00	20.75	47.96	37.98	19.31	30.28	32.41
LLaVA-Med-7B [18]	27.79	25.86	24.04	33.69	25.11	25.96	26.17	33.36	27.75
MedVLM-R1-2B [32]	16.27	15.42	15.32	36.32	14.08	19.43	8.33	35.56	20.09
HealthGPT-M3-3.8B [23]	21.63	10.87	26.58	20.23	15.35	12.41	16.06	23.97	18.39
HeartcareGPT-3.8B	<u>81.95</u>	<u>95.94</u>	<u>82.79</u>	79.84	<u>87.85</u>	92.21	<u>79.25</u>	<u>67.80</u>	<u>83.33</u>
HeartcareGPT-7B	86.16	98.62	93.20	<u>75.15</u>	62.71	<u>87.82</u>	85.13	78.59	83.42

Table 2. Performance comparison between HeartcareGPT and baselines on the *open-QA* task from Heartcare-Bench^S and Heartcare-Bench^I.

Model	Heartcare-Bench ^S								Heartcare-Bench ^I							
	Diagnosis		Waveform		Rhythm		Misc.		Diagnosis		Waveform		Rhythm		Misc.	
	F1-Bio	Rouge-L	F1-Bio	Rouge-L	F1-Bio	Rouge-L	F1-Bio	Rouge-L	F1-Bio	Rouge-L	F1-Bio	Rouge-L	F1-Bio	Rouge-L	F1-Bio	Rouge-L
<i>Generalist Models</i>																
LLaVA-1.5-7B [24]	18.52	11.57	25.34	13.93	20.84	12.45	27.53	14.82	14.82	10.25	11.24	9.67	17.53	11.38	24.21	13.76
Qwen2.5-VL-7B [5]	27.63	12.84	34.15	15.72	30.82	13.96	34.27	16.38	35.24	14.93	30.35	13.27	21.84	12.18	40.13	17.24
InternVL-2.5-8B [10]	29.27	13.29	33.52	14.86	30.64	13.72	39.82	16.95	25.37	11.82	17.26	10.45	37.53	15.63	39.27	16.84
Yi-VL-6B [47]	48.53	15.38	38.27	14.72	30.42	13.85	38.96	15.63	58.92	17.82	43.85	16.27	16.43	10.84	38.74	15.49
MiniCPM-V2.6-8B [12]	31.84	12.93	30.73	12.84	22.86	11.75	31.52	13.92	23.17	11.28	32.94	13.46	9.53	8.67	29.83	13.27
Gemma-3-4B [39]	12.90	5.49	11.57	6.95	13.85	5.87	23.01	6.08	14.13	6.65	14.74	9.90	15.12	5.95	21.02	8.98
Claude-3.5 [1]	21.43	5.04	14.81	4.36	23.01	6.75	17.23	7.91	21.43	5.39	27.69	5.02	17.78	4.13	19.14	10.24
GPT5 [31]	23.00	7.25	21.42	13.93	37.39	14.71	24.83	9.57	40.82	15.93	33.52	12.84	33.17	12.53	25.64	9.82
<i>Medical Models</i>																
Lingshu-7B [44]	28.94	12.37	32.84	14.26	39.27	15.84	20.17	10.53	47.36	16.28	37.35	15.12	18.74	10.87	29.63	13.15
LLaVA-Med-7B [18]	27.15	12.84	25.27	11.93	23.48	11.27	33.02	14.38	24.53	11.29	25.37	12.15	25.53	11.84	32.74	14.26
MedVLM-R1-2B [32]	15.64	8.73	14.83	8.25	14.73	8.16	35.64	13.52	13.52	7.84	18.84	9.27	16.83	6.45	34.92	13.17
HealthGPT-M3-3.8B [23]	21.07	10.82	10.27	8.93	25.94	11.76	19.63	10.24	14.83	9.67	11.84	8.75	15.43	9.82	23.37	11.39
HeartcareGPT-3.8B	<u>68.53</u>	<u>32.27</u>	<u>72.74</u>	<u>35.38</u>	78.63	36.42	<u>65.84</u>	<u>30.97</u>	<u>63.17</u>	<u>29.83</u>	<u>70.92</u>	33.57	75.36	34.69	<u>61.53</u>	<u>28.24</u>
HeartcareGPT-7B	72.94	36.85	78.26	39.64	<u>73.62</u>	<u>35.27</u>	68.37	34.18	67.43	33.52	76.73	37.84	<u>69.84</u>	<u>32.47</u>	64.17	31.73

7. Conclusion

Heartcare Suite establishes a comprehensive multimodal foundation framework for fine-grained ECG understanding, integrating high-quality dataset, clinically aligned benchmarks, and scalable modeling strategies. We hope this work serves as a stepping stone for future research on Med-LLMs in clinically grounded signal-language reasoning.

References

- [1] Anthropic. Claude 3.5. <https://www.anthropic.com>, 2024. Large Language Model by Anthropic. 1, 6, 8, 9
- [2] Raymond Ao and George He. Image based deep learning in 12-lead ecg diagnosis. *Frontiers in Artificial Intelligence*, 5: 1087370, 2023. 2
- [3] Anas Awadalla, Irena Gao, Josh Gardner, Jack Hessel, Yusuf Hanafy, Wanrong Zhu, Kalyani Marathe, Yonatan Bitton, Samir Gadre, Shiori Sagawa, et al. Openflamingo: An open-

source framework for training large autoregressive vision-language models. *arXiv preprint arXiv:2308.01390*, 2023. 1

- [4] Ahtisham Ayyub, Christos Politis, and Muhammad Arslan Usman. A comprehensive review of ai-based detection of arrhythmia using electrocardiogram (ecg). *Computers in Biology and Medicine*, 196:110594, 2025. 1
- [5] Shuai Bai, Keqin Chen, Xuejing Liu, Jialin Wang, Wenbin Ge, Sibao Song, Kai Dang, Peng Wang, Shijie Wang, Jun Tang, et al. Qwen2. 5-vl technical report. *arXiv preprint arXiv:2502.13923*, 2025. 1, 6, 8, 9
- [6] Mingsheng Cai, Jiuming Jiang, Wenhao Huang, Che Liu, and Rossella Arcucci. Supreme: A supervised pre-training framework for multimodal ecg representation learning. *arXiv preprint arXiv:2502.19668*, 2025. 3
- [7] Juan Manuel Zambrano Chaves, Shih-Cheng Huang, Yanbo Xu, Hanwen Xu, Naoto Usuyama, Sheng Zhang, Fei Wang, Yujia Xie, Mahmoud Khademi, Ziyi Yang, et al. Towards a clinically accessible radiology foundation model: open-

Table 3. Performance comparison between HeartcareGPT and other baselines on the *Comparison-QA* task from our proposed Heartcare-Bench^C. Cons. = Consecutive ECGs from the same patient; Irr. = Irrelevant ECGs from different patients. Yi-VL-6B and HealthGPT-M3-3.8B do not support multi-image input.

Model	S-S		I-I		S-I		Avg.
	Cons.	Irr.	Cons.	Irr.	Cons.	Irr.	
<i>Generalist Models</i>							
LLaVA-1.5-7B [24]	62.70	56.24	66.17	63.51	47.94	45.65	57.04
Qwen2.5-VL-7B [5]	50.64	47.26	49.36	50.68	50.21	51.28	49.91
InternVL-2.5-8B [10]	47.83	45.13	46.18	43.33	49.40	43.24	45.85
MiniCPM-V2.6-8B [12]	53.22	48.13	51.87	45.50	49.85	45.05	48.97
Gemma-3-4B [39]	49.18	38.53	49.63	35.44	49.55	35.59	42.99
Claude-3.5 [1]	46.17	43.96	39.15	56.78	24.47	54.82	44.23
GPT5 [31]	50.97	49.18	50.82	49.40	50.00	47.90	49.71
<i>Medical Models</i>							
Lingshu-7B [44]	58.79	45.01	62.13	59.46	45.11	43.12	52.27
LLaVA-Med-7B [18]	35.46	34.82	32.84	32.65	43.26	34.14	35.53
MedVLM-R1-2B [32]	58.44	39.33	53.69	40.34	49.57	37.95	46.55
HeartcareGPT-3.8B	<u>66.40</u>	<u>67.47</u>	<u>69.88</u>	<u>75.19</u>	<u>78.71</u>	<u>78.83</u>	<u>72.74</u>
HeartcareGPT-7B	74.01	75.87	74.80	79.09	80.05	79.55	77.23

Table 4. Performance comparison between HeartcareGPT and other baseline methods on the *report generation* task from our proposed Heartcare-Bench^S and Heartcare-Bench^I.

Model	Heartcare-Bench ^S			Heartcare-Bench ^I		
	Score ^{GPT}	F1-Rad	Rouge-L	Score ^{GPT}	F1-Rad	Rouge-L
<i>Generalist Models</i>						
LLaVA-1.5-7B [24]	55.69	5.22	18.30	37.40	12.90	20.75
Qwen2.5-VL-7B [5]	<u>64.60</u>	5.64	9.00	<u>67.40</u>	7.67	13.56
InternVL-2.5-8B [10]	42.07	5.50	9.13	33.69	7.73	11.02
Yi-VL-6B [47]	26.58	3.75	13.05	21.74	6.73	15.18
MiniCPM-V2.6-8B [12]	34.54	5.74	10.66	49.60	7.48	12.63
Gemma-3-4B [39]	64.57	4.38	7.57	57.10	7.00	9.07
Claude-3.5 [1]	63.11	5.03	12.33	63.29	7.63	14.02
GPT5 [31]	62.73	4.85	8.86	78.80	6.29	9.55
<i>Medical Models</i>						
xu2025lingshu Lingshu-7B [44]	58.89	7.13	13.94	51.94	9.52	16.31
LLaVA-Med-7B [18]	50.02	5.21	14.95	27.71	6.56	16.45
MedVLM-R1-2B [32]	32.26	2.10	15.51	56.58	9.05	18.27
HealthGPT-M3-3.8B [23]	25.39	1.00	7.53	37.62	1.22	9.13
HeartcareGPT-3.8B	61.29	26.84	34.39	78.50	<u>23.10</u>	<u>38.68</u>
HeartcareGPT-7B	76.55	<u>21.70</u>	<u>32.55</u>	65.03	27.17	44.86

access and lightweight, with automated evaluation. *arXiv preprint arXiv:2403.08002*, 2024. 3

- [8] Chen Chen, Lei Li, Marcel Beetz, Abhirup Banerjee, Rameek Gupta, and Vicente Grau. Large language model-informed ecg dual attention network for heart failure risk prediction. *IEEE Transactions on Big Data*, 2025. 3
- [9] Junying Chen, Chi Gui, Ruyi Ouyang, Anningzhe Gao, Shunan Chen, Guiming Hardy Chen, Xidong Wang, Ruifei Zhang, Zhenyang Cai, Ke Ji, et al. Huatuoqpt-vision, towards injecting medical visual knowledge into multimodal llms at scale. *arXiv preprint arXiv:2406.19280*, 2024. 1, 3
- [10] Zhe Chen, Weiyun Wang, Yue Cao, Yangzhou Liu, Zhangwei Gao, Erfei Cui, Jinguo Zhu, Shenglong Ye, Hao Tian, Zhaoyang Liu, et al. Expanding performance boundaries of open-source multimodal models with model, data, and test-time scaling. *arXiv preprint arXiv:2412.05271*, 2024. 1, 6, 8,

9

- [11] Patrick Esser, Robin Rombach, and Bjorn Ommer. Taming transformers for high-resolution image synthesis. In *Proceedings of the IEEE/CVF conference on computer vision and pattern recognition*, pages 12873–12883, 2021. 2
- [12] Shengding Hu, Yuge Tu, Xu Han, Chaoqun He, Ganqu Cui, Xiang Long, Zhi Zheng, Yewei Fang, Yuxiang Huang, Weilin Zhao, et al. Minicpm: Unveiling the potential of small language models with scalable training strategies. *arXiv preprint arXiv:2404.06395*, 2024. 6, 8, 9
- [13] John D Hunter. Matplotlib: A 2d graphics environment. *Computing in Science & Engineering*, 9(3):90–95, 2007. 12
- [14] Artifex Software Inc. Pymupdf: Python bindings for mupdf – a lightweight pdf and xps viewer. <https://github.com/pymupdf/PyMuPDF>, 2024. Accessed: 2025-05-16. 12
- [15] Saahil Jain, Ashwin Agrawal, Adriel Saporta, Steven QH Truong, Du Nguyen Duong, Tan Bui, Pierre Chambon, Yuhao Zhang, Matthew P Lungren, Andrew Y Ng, et al. Radgraph: Extracting clinical entities and relations from radiology reports. *arXiv preprint arXiv:2106.14463*, 2021. 14
- [16] Songtao Jiang, Tuo Zheng, Yan Zhang, Yeying Jin, Li Yuan, and Zuozhu Liu. Med-moe: Mixture of domain-specific experts for lightweight medical vision-language models, 2024. 3
- [17] Jiarui Jin, Haoyu Wang, Hongyan Li, Jun Li, Jiahui Pan, and Shenda Hong. Reading your heart: Learning ecg words and sentences via pre-training ecg language model. *arXiv preprint arXiv:2502.10707*, 2025. 3
- [18] Chunyuan Li, Cliff Wong, Sheng Zhang, Naoto Usuyama, Haitian Liu, Jianwei Yang, Tristan Naumann, Hoifung Poon, and Jianfeng Gao. Llava-med: Training a large language-and-vision assistant for biomedicine in one day. *Advances in Neural Information Processing Systems*, 36:28541–28564, 2023. 1, 3, 6, 8, 9
- [19] Junnan Li, Dongxu Li, Silvio Savarese, and Steven Hoi. Blip-2: Bootstrapping language-image pre-training with frozen image encoders and large language models. In *International conference on machine learning*, pages 19730–19742. PMLR, 2023. 1
- [20] Sijing Li, Tianwei Lin, Lingshuai Lin, Wenqiao Zhang, Jiang Liu, Xiaoda Yang, Juncheng Li, Yucheng He, Xiaohui Song, Jun Xiao, et al. Eyecaregpt: Boosting comprehensive ophthalmology understanding with tailored dataset, benchmark and model. *arXiv preprint arXiv:2504.13650*, 2025. 3
- [21] Xihong Lian, Limin Jiao, Zejin Liu, Qiqi Jia, Jing Zhong, Miao Fang, and Weilin Wang. Multi-spatiotemporal heterogeneous legacy effects of climate on terrestrial vegetation dynamics in china. *GIScience & Remote Sensing*, 59(1): 164–183, 2022. 2
- [22] Chin-Yew Lin. Rouge: A package for automatic evaluation of summaries. In *Text summarization branches out: Proceedings of the ACL-04 workshop*, pages 74–81. Association for Computational Linguistics, 2004. 14
- [23] Tianwei Lin, Wenqiao Zhang, Sijing Li, Yuqian Yuan, Binhe Yu, Haoyuan Li, Wanggui He, Hao Jiang, Mengze Li, Xiaohui Song, et al. Healthgpt: A medical large vision-language model for unifying comprehension and generation

- via heterogeneous knowledge adaptation. *arXiv preprint arXiv:2502.09838*, 2025. 1, 3, 6, 8, 9
- [24] Haotian Liu, Chunyuan Li, Qingyang Wu, and Yong Jae Lee. Visual instruction tuning. *Advances in neural information processing systems*, 36:34892–34916, 2023. 1, 8, 9
- [25] Dominique Makowski and contributors. Neurokit2: Python toolbox for neurophysiological signal processing. <https://github.com/neuropsychology/NeuroKit>, 2024. Accessed: 2025-05-16. 12
- [26] Michael Moor, Qian Huang, Shirley Wu, Michihiro Yasunaga, Yash Dalmia, Jure Leskovec, Cyril Zakka, Eduardo Pontes Reis, and Pranav Rajpurkar. Med-flamingo: a multimodal medical few-shot learner. In *Machine Learning for Health (ML4H)*, pages 353–367. PMLR, 2023. 1, 3
- [27] Yoojin Nam, Dong Yeong Kim, Sunggu Kyung, Jinyoung Seo, Jeong Min Song, Jimin Kwon, Jihyun Kim, Wooyoung Jo, Hyungbin Park, Jimin Sung, et al. Multimodal large language models in medical imaging: Current state and future directions. *Korean Journal of Radiology*, 26(10):900, 2025. 1
- [28] Cuong V Nguyen, Hieu X Nguyen, Dung D Pham Minh, and Cuong D Do. Comparing deep neural network for multi-label ecg diagnosis from scanned ecg. *arXiv preprint arXiv:2502.14909*, 2025. 2
- [29] Jungwoo Oh, Gyubok Lee, Seongsu Bae, Joon myoung Kwon, and Edward Choi. Ecg-qa: A comprehensive question answering dataset combined with electrocardiogram, 2023. 3, 4
- [30] OpenAI. Gpt-4v(ision) system card. https://cdn.openai.com/papers/GPTV_System_Card.pdf, 2023. 1, 12, 14
- [31] OpenAI. Gpt-5 system card. <https://https://cdn.openai.com/gpt-5-system-card.pdf>, 2023. 6, 8, 9
- [32] Jiazhen Pan, Che Liu, Junde Wu, Fenglin Liu, Jiayuan Zhu, Hongwei Bran Li, Chen Chen, Cheng Ouyang, and Daniel Rueckert. Medvlm-r1: Incentivizing medical reasoning capability of vision-language models (vlms) via reinforcement learning. *arXiv preprint arXiv:2502.19634*, 2025. 3, 6, 8, 9
- [33] Zhiliang Peng, Wenhui Wang, Li Dong, Yaru Hao, Shaohan Huang, Shuming Ma, and Furu Wei. Kosmos-2: Grounding multimodal large language models to the world. *arXiv preprint arXiv:2306.14824*, 2023. 1
- [34] Eedara Prabhakararao and Samarendra Dandapt. Multi-label ecg classification using temporal convolutional neural network. *arXiv preprint arXiv:2306.03844*, 2023. 2
- [35] Lance A Ramshaw and Mitchell P Marcus. Text chunking using transformation-based learning. In *Natural language processing using very large corpora*, pages 157–176. Springer, 1999. 14
- [36] Ikaros Silva. Wfdb app toolbox for matlab/octave. <https://github.com/ikarosilva/wfdb-app-toolbox>, 2023. Accessed: 2025-05-16. 12
- [37] Nils Strodthoff, Patrick Wagner, Tobias Schaeffter, and Wojciech Samek. Deep learning for ecg analysis: Benchmarks and insights from ptb-xl. *IEEE journal of biomedical and health informatics*, 25(5):1519–1528, 2020. 2
- [38] Kai Sun, Siyan Xue, Fuchun Sun, Haoran Sun, Yu Luo, Ling Wang, Siyuan Wang, Na Guo, Lei Liu, Tian Zhao, et al. Medical multimodal foundation models in clinical diagnosis and treatment: Applications, challenges, and future directions. *arXiv preprint arXiv:2412.02621*, 2024. 1
- [39] Gemma Team, Aishwarya Kamath, Johan Ferret, Shreya Pathak, Nino Vieillard, Ramona Merhej, Sarah Perrin, Tatiana Matejovicova, Alexandre Ramé, Morgane Rivière, et al. Gemma 3 technical report. *arXiv preprint arXiv:2503.19786*, 2025. 1, 6, 8, 9
- [40] Eric J Topol. High-performance medicine: the convergence of human and artificial intelligence. *Nature medicine*, 25(1): 44–56, 2019. 1
- [41] Aaron Van Den Oord, Oriol Vinyals, et al. Neural discrete representation learning. *Advances in neural information processing systems*, 30, 2017. 2
- [42] Patrick Wagner, Nils Strodthoff, Ralf-Dieter Boussejot, Dieter Kreiseler, Fatima I Lunze, Wojciech Samek, and Tobias Schaeffter. Ptb-xl, a large publicly available electrocardiography dataset. *Scientific data*, 7(1):1–15, 2020. 1, 2
- [43] Liping Xie, Zilong Li, Yihan Zhou, Yiliu He, and Jiaxin Zhu. Computational diagnostic techniques for electrocardiogram signal analysis. *Sensors*, 20(21):6318, 2020. 1
- [44] Weiwen Xu, Hou Pong Chan, Long Li, Mahani Aljunied, Ruifeng Yuan, Jianyu Wang, Chenghao Xiao, Guizhen Chen, Chaoqun Liu, Zhaodonghui Li, et al. Lingshu: A generalist foundation model for unified multimodal medical understanding and reasoning. *arXiv preprint arXiv:2506.07044*, 2025. 1, 3, 6, 8, 9
- [45] Kai Yang, Massimo Hong, Jiahuan Zhang, Yizhen Luo, Suyuan Zhao, Ou Zhang, Xiaomao Yu, Jiawen Zhou, Liuqing Yang, Ping Zhang, et al. Ecg-lm: Understanding electrocardiogram with a large language model. *Health Data Science*, 5:0221, 2025. 3
- [46] Jiabo Ye, Haiyang Xu, Haowei Liu, Anwen Hu, Ming Yan, Qi Qian, Ji Zhang, Fei Huang, and Jingren Zhou. mplug-owl3: Towards long image-sequence understanding in multi-modal large language models. *arXiv preprint arXiv:2408.04840*, 2024. 1
- [47] Alex Young, Bei Chen, Chao Li, Chengen Huang, Ge Zhang, Guanwei Zhang, Guoyin Wang, Heng Li, Jiangcheng Zhu, Jianqun Chen, et al. Yi: Open foundation models by 01. ai. *arXiv preprint arXiv:2403.04652*, 2024. 1, 6, 8, 9
- [48] Han Yu, Huiyuan Yang, and Akane Sano. Ecg-sl: Electrocardiogram (ecg) segment learning, a deep learning method for ecg signal. *arXiv preprint arXiv:2310.00818*, 2023. 3
- [49] Han Yu, Peikun Guo, and Akane Sano. Ecg semantic integrator (esi): A foundation ecg model pretrained with llm-enhanced cardiological text. *arXiv preprint arXiv:2405.19366*, 2024. 3
- [50] Neil Zeghidour, Alejandro Luebs, Ahmed Omran, Jan Skoglund, and Marco Tagliasacchi. Soundstream: An end-to-end neural audio codec. *IEEE/ACM Transactions on Audio, Speech, and Language Processing*, 30:495–507, 2021. 2
- [51] Xiaohua Zhai, Basil Mustafa, Alexander Kolesnikov, and Lucas Beyer. Sigmoid loss for language image pre-training, 2023. 6

- [52] Yutong Zhang, Yi Pan, Tianyang Zhong, Peixin Dong, Kangni Xie, Yuxiao Liu, Hanqi Jiang, Zihao Wu, Zhengliang Liu, Wei Zhao, et al. Potential of multimodal large language models for data mining of medical images and free-text reports. *Meta-Radiology*, 2(4):100103, 2024. [1](#)
- [53] Juexiao Zhou, Xiaonan He, Liyuan Sun, Jiannan Xu, Xiuying Chen, Yuetan Chu, Longxi Zhou, Xingyu Liao, Bin Zhang, and Xin Gao. Skingpt-4: an interactive dermatology diagnostic system with visual large language model. *arXiv preprint arXiv:2304.10691*, 2023. [3](#)

Appendix

This is the Appendix for "HeartcareGPT: A Unified Multimodal ECG Suite for Dual Signal-Image Modeling and Understanding".

This Appendix is organized as follows:

- Section A provides the details of our proposed multimodal data engine—**HeartAgent**.
- Section B provides the details of the experimental implementation, the training process of **HeartcareGPT**, the construction details of **Heartcare-400K**, and the specific information of **Heartcare-Bench**.
- Section C shows our detailed ablation experimental results of **HeartcareGPT** and **Beat**.
- Section D shows typical data examples in **Heartcare-400K**.
- Section E lists the broader impact and limitations of this paper.

A. Multimodal Data Engine Details

To efficiently construct the Heartcare-400K dataset, we design **HeartAgent**, an automated multimodal data engine that transforms multi-source ECG data into high-quality, structured VQA pairs. As illustrated in Figure 2, the system consists of four core modules that work collaboratively to complete the full pipeline from raw data parsing to task QA generation.

Multimodal Feature Converter. The Converter preprocesses hospital PDF reports into standardized inputs for downstream modules. It extracts patient metadata (e.g., age, sex) and diagnostic details (diagnosis, waveform, rhythm and other features) from the PDF via fitz (PyMuPDF)[14] and regular expressions. Subsequently, diagnostic text is mapped to structured English labels in accordance with the SCP-ECG semantic standard.

Noise Filtering and Quality Optimizer. The Optimizer implements a parsing mechanism to unify heterogeneous ECG inputs into standardized 12-lead, 250 Hz digital signals. Structured digital inputs from public datasets are processed via the WFDB toolkit [36]. To correct noise, drift, and missing-segment issues, the Optimizer applies a three-stage enhancement pipeline: (i) resampling all signals to 250 Hz, (ii) applying NeuroKit2’s clean function for lead-level denoising and baseline correction, and (iii) using NeuroKit2’s quality scores [25] to extract high-quality segments while discarding low-quality regions.

Diversed Image Generator. The Image Generator processes clear waveform images through a dual-channel pipeline. For high-quality signals originated from the Optimizer, the Generator uses Matplotlib[13] in the final stage to render the clean digital signals into images. For hospital reports, it processes PDF-based reports to produce cropped images

of the complete 12-lead tracings, while ensuring all data is de-identified.

Multi-Task QA Builder. To enhance model generalization and training consistency across multi-level ECG VQA scenarios, we use GPT-4 [30] to directly generate structured multimodal ECG QA samples, constructing the training dataset. Each generated sample consists of four key components: (i) **Context Description**, providing background information such as patient demographics, signal snippets, or clinical report summaries; (ii) **Task Instruction**, specifying the required operation type, including multiple-choice QA, open-ended QA, report generation, or waveform prediction; (iii) **Auxiliary Labels**, providing additional structured supervisory information to enhance training quality; and (iv) **Output Format**, standardizing expression of answers to ensure consistency across tasks.

B. Implementation Details

B.1. Model Details

HeartcareGPT employs an architecture design that aligns ECG signals and images with textual inputs in latent space. For signal and image modalities, We use two MLP projectors for cross-modal feature fusion. Notably, we implement LoRA for parameter-efficient fine-tuning, preserving pre-trained knowledge while enabling domain-specific adaptation for ECG tasks. This design achieves an optimal balance between model capacity and computational efficiency, establishing a scalable architectural foundation for multimodal ECG understanding.

HeartcareGPT offers two versions: **HeartcareGPT-3.8B** and **HeartcareGPT-7B**, which are based on Phi-3-Mini-4K-Instruct and Qwen2.5-7B-Instruct as the pre-trained LLMs, respectively. We extend the model’s native textual tokenizer by adding five special tokens: `<PREDICTION>`, `<SIGNAL_START>`, `<SIGNAL_END>`, `<IMAGE_START>`, and `<IMAGE_END>`. The `<PREDICTION>` token indicates that the model is expected to perform signal-prediction tasks handled by the integrated beat module. `<SIGNAL_START>` and `<SIGNAL_END>` mark the boundaries of signal embeddings, and `<IMAGE_START>` and `<IMAGE_END>` mark the boundaries of image embeddings, enabling the model to more reliably recognize and process these modality-specific representations. Table 5 shows the details.

In addition, for baseline models that support only a single input modality, we apply a unified preprocessing strategy to align modalities, ensuring fairness within the same evaluation framework. These baseline models typically support only image inputs rather than raw signals. Therefore, we convert the ECG signals into images using the Diverse Image Generator module of HeartAgent (presented in Appendix A), and feed the generated images together with the textual ques-

Table 5. Overview of the components of HeartcareGPT.

Model	ViT	Signal Projector	Image Projector	LLM	Params	Vocab Size	LoRA Rank
HeartcareGPT-3.8B	SigLIP-So400M-patch14-384	1-layer MLP	2-layer MLP	Phi-3-Mini-4K-Instruct	3.8B	32,069	64
HeartcareGPT-7B	SigLIP-So400M-patch14-384	1-layer MLP	2-layer MLP	Qwen2.5-7B-Instruct	7B	151,851	64

tions into the baseline models to obtain their responses.

B.2. Training Details

We follow a three-stage training paradigm: (i) training Beat to extract high-fidelity ECG embeddings, (ii) warming up the visual and signal projectors to stabilize feature alignment, and (iii) performing joint instruction fine-tuning on Heartcare-400K for end-to-end modeling. This paradigm achieves decoupled feature learning and semantic alignment across stages, enabling the model to maintain signal fidelity while acquiring advanced clinical reasoning capabilities.

Training Beat. Beat is first trained on PTB-XL dataset. We use a joint supervision strategy to optimize reconstruction and prediction losses simultaneously. This stage focuses on learning robust ECG signal representations through DVQ structure.

Warming Up. We warm up the visual and signal projectors using paired ECG images and signals, allowing the model to align heterogeneous features in a controlled manner. By isolating projector optimization from the LLM, the model avoids early-stage instability and catastrophic feature distortion. This step establishes a coherent multimodal latent space for unified processing.

Joint Fine-Tuning. We perform full-model instruction fine-tuning on Heartcare-400K, enabling the LLM to associate ECG inputs with diagnostic reasoning, structured reporting, and question answering. The model learns both high-level clinical knowledge and fine-grained ECG interpretation skills. This stage integrates all modalities end-to-end, yielding a clinically aligned and diagnostically capable ECG foundation model.

Hyperparameter configurations for each training stage are detailed in Table 6.

B.3. Construction details of Heartcare-400K

Data Source Details. In the data collection phase, we gather ECG report data with two modalities - digitized raw signals and clinical report images.

PTB-XL is one of the largest publicly available electrocardiogram datasets, comprising 21,799 clinical 12-lead ECG recordings that cover a diverse range of cardiac pathologies as well as healthy control data. Each recording has a duration of 10 seconds with a sampling rate of 500 Hz, accompanied by standardized diagnostic annotations and detailed patient metadata, such as gender and age. We utilize PTB-XL as a high-quality structured data source to enhance the diversity and accuracy of Heartcare-400K in the digital modality.

In contrast, ECG image modality data has long been constrained by acquisition challenges, annotation costs, and privacy concerns, resulting in scarce and outdated publicly available image datasets. To address this issue, we establish collaborations with two top-tier hospitals and collect a total of 12,170 recent ECG report forms through rigorous anonymization and professional physician annotations. Each report is in a standardized PDF format, containing basic patient information, physiological parameters, physician diagnoses, and approximately 5-second 12-lead image recordings, significantly improving the timeliness and clinical usability of the image modality.

To provide a comprehensive overview of the diagnostic coverage and clinical relevance of Heartcare-400K, Table 7 presents a detailed listing of ECG features organized across four clinically critical dimensions: (i) Diagnosis (e.g., Inferior MI, AV block), (ii) Waveform abnormalities (e.g., T abnormalities, ST depression), (iii) Rhythm patterns (e.g., sinus rhythm, atrial fibrillation), and (iv) Miscellaneous features (e.g., noise, heart axis). This illustrates the dataset’s comprehensive and balanced representation across these clinically relevant dimensions.

To visually summarize the dataset composition and task-specific coverage of Heartcare-400K, we provide a hierarchical radial visualization in Figure 6. This depicts the distribution of QA subtasks within three benchmarks, Heartcare-Bench^S, Heartcare-Bench^I and Heartcare-Bench^C, highlighting both the relative scale and fine-grained breakdown of different data types.

QA Templates. For datasets that only contain classification or grading labels, we analyze the data characteristics of their labels and design different Question-Answering (QA) templates for each. This allows us to transform the original data into QA pairs. We additionally provide the prompt used to guide GPT-4 in generating QA templates for the diagnostic subtask in the closed-QA data construction pipeline of HeartAgent, as shown in Figure 7. Examples of the QA templates are shown in the Table 8.

B.4. Construction details of Heartcare-Bench

To comprehensively assess model performance across different task types, we design a multi-dimensional evaluation framework tailored to the specific objectives of each module. The evaluation criteria are carefully selected to reflect the core competencies required by each task—ranging from answer correctness and semantic understanding to clinical accuracy and waveform forecasting fidelity.

Table 6. Overview of hyperparameter configurations. Stage 1 = Training Beat; Stage 2 = Warming up; Stage 3 = Joint fine-tuning.

Hyperparameter	HeartcareGPT-3.8B			HeartcareGPT-7B		
	Training Beat	Warming up	Joint Fine-Tuning	Training Beat	Warming up	Joint Fine-Tuning
Optimizer	AdamW	AdamW	AdamW	AdamW	AdamW	AdamW
Adapter LR	/	/	2e-5	/	/	2e-5
Learning Rate	1e-4	2e-4	2e-5	1e-4	2e-4	2e-5
Global Batch Size	32	16	16	32	16	16
Weight Decay	0	0.01	0.01	0	0.01	0.01
Dropout Rate	0	0	0.05	0	0	0.05
LR Scheduler	Cosine Annealing	Linear	Linear	Cosine Annealing	Linear	Linear

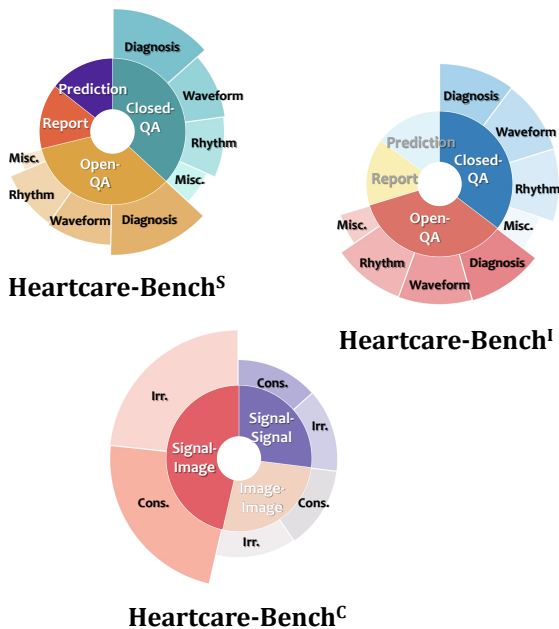


Figure 6. Hierarchical distribution of Heartcare-400K dataset across benchmarks and subtask types.

Closed-QA. We measure model discrimination performance by standard *Accuracy*.

Open-QA. We adopt a dual-track evaluation comprising (i) *F1-Bio*[35] to assess semantic alignment, and (ii) *ROUGE-L*[22] to quantify linguistic fluency and contextual style fidelity.

Comparison-QA. We measure model discrimination performance by standard *Accuracy*.

Report Generation. (i) Beyond ROUGE-L, we use *F1-RadGraph*[15] to evaluate the precision of entity and relation extraction in the report structure. To capture ECG-specific correctness, we introduce three medical-key indicators—*diagnosis completeness*, *waveform feature recognition accuracy*, and *rhythm classification accuracy*. (ii) We implement a 100-point, multi-dimensional rubric that evaluates diagnos-

tic completeness, linguistic conformity, structural coherence, and privacy protection. Using GPT-4[30], we tally error types and severity according to this rubric (see Table 9 for weighted penalties). The template used for GPT-4’s evaluation is shown in Figure 8. According to the evaluation criteria, we grade the reports as follows:

- **Excellent Report (90-100):** Nearly error-free with complete diagnostic information, clear structure, and no clinically significant mistakes. Ready for immediate clinical use.
- **Acceptable Report (80-89):** Contains minor errors but maintains diagnostic accuracy and logical flow. Requires minimal editing before clinical application.
- **Review Required Report (60-79):** Has notable errors, incomplete information, or unclear structure. Needs expert verification before use.
- **Unusable Report (< 60):** Contains critical errors, major missing information, or serious diagnostic inaccuracies. Unsafe for clinical decision-making.

Signal Prediction. We delimit the predicted segment the with special token <PREDICTION> and compute the *Mean Squared Error (MSE)* between the forecasted waveform and the true continuation. Lower MSE indicates superior prediction accuracy.

Heartcare-Bench adopts strict patient-level partitioning to ensure that all ECG records from the same individual—across different visits, formats, or tasks—reside in a single split. To further eliminate potential leakage, we perform a lightweight yet comprehensive overlap check that includes: (i) examination-level matching using study IDs and timestamps, (ii) duplicate detection of ECG waveforms via normalized hashing, and (iii) visual/textual duplication inspection for rendered ECG images and associated reports. These checks jointly guarantee that no record, waveform, or derived annotation appears across splits, ensuring fair and leakage-free evaluation.

Closed-QA Generation Prompt of Diagnosis

System Prompt:

You will be given structured ECG-related variables (age, gender, and a diagnosis-probability JSON). Your task is to generate exactly one JSON object that represents a single **Diagnosis Closed-QA** item. The output must contain the fields "type", "question", and "answer", and must follow all rules specified below. No additional commentary, explanations, or extra text is allowed.

Instruction:

- **Age:** {Integer}
- **Gender:** {Male / Female / Other}
- **Diagnosis Type:** {DIAGNOSIS_TYPE_JSON}

Each key of the diagnosis type JSON is a possible diagnosis and value is a probability (0–100). For example:

```
{
  "Inferior myocardial infarction": 95.0,
  "Atrial fibrillation": 30.0
}
```

If no diagnoses are present, it is an empty JSON.

• Rules for Using Probabilities:

1. If there is at least one diagnosis ≥ 60 , choose the highest-probability diagnosis as the correct option.
2. If all diagnosis < 60 , and the diagnosis type JSON is only composed of low-probability values or empty, then the correct answer must be one "Normal" expression.
3. A "Normal" option may be included when it is not the correct answer, and its wording can follow any standard clinical phrasing indicating normal findings (e.g., expressions such as "Normal ECG", "Within normal limits", or equivalent variants).
4. Distractors must be clinically plausible but must not overlap with any actual diagnosis in the diagnosis type JSON.

• Requirements:

1. The "question" field must be a single string and must mention both the patient's age and gender. The phrasing should vary naturally. For example:
 - "Based on the ECG signal of a 65-year-old male patient, ..."
 - "For the ECG of a 70-year-old female, ..."
 - "This ECG from a 55-year-old male patient indicates ..."
 - "Considering the ECG tracing of a 60-year-old patient (female), ..."
2. The question text must include ONLY four options labeled "A: ...; B: ...; C: ...; D: ..." (separated by semicolons), e.g., "Based on the ECG signal of a 65-year-old male patient, Which diagnosis is most likely? A: Atrial fibrillation; B: No abnormality detected; C: Inferior myocardial infarction; D: Complete right bundle branch block".
3. The "answer" field must be exactly the option label plus content, e.g., "A: Atrial fibrillation".
4. The correct answer must not consistently appear in the same option position; its placement among A–D should be randomized.
5. The output must be in the form of JSON:

```
{
  "type": "DiagnosisClosedQA",
  "question": "...",
  "answer": "...",
}
```

Figure 7. Prompt for QA pairs generation in *closed-QA* tasks, diagnosis dimension.

Table 7. Systematic Categorization of ECG Features in Heartcare-400K.

Diagnosis	
ischemic in inferior leads	non-specific ischemic
septal hypertrophy	non-specific intraventricular conduction block
subendocardial injury in anterolateral leads	left anterior fascicular block
ischemic in anterior leads	non-diagnostic T abnormalities
anterolateral myocardial infarction	incomplete right bundle branch block
non-specific ST changes	third degree AV block
right ventricular hypertrophy	ischemic in lateral leads
incomplete left bundle branch block	long QTc-interval
first degree AV block	inferoposterior myocardial infarction
right atrial hypertrophy	Wolf-Parkinson-White syndrome
subendocardial injury in anteroseptal leads	inferolateral myocardial infarction
inferior myocardial infarction	posterior myocardial infarction
right atrial overload/enlargement	long QT-interval
complete left bundle branch block	left posterior fascicular block
intraventricular conduction block	complete right bundle branch block
inferoposterolateral myocardial infarction	ST-T changes compatible with ventricular aneurysm
left atrial overload/enlargement	ischemic in inferolateral leads
digitalis-effect	anterior myocardial infarction
ischemic in anterolateral leads	subendocardial injury in lateral leads
subendocardial injury in inferolateral leads	subendocardial injury in inferior leads
biatrial hypertrophy	second degree AV block
left ventricular hypertrophy	lateral myocardial infarction
ischemic in anteroseptal leads	anteroseptal myocardial infarction
electrolytic disturbance or drug	ST-T changes
Waveform	
non-specific ST changes	low QRS voltage in chest leads
low QRS voltage in limb leads	Q waves present
low QRS voltage in left chest leads	long QTc-interval
long QT-interval	digitalis-effect
non-specific ST elevation	high QRS voltage in left ventricular
low QRS voltage in chest and limb leads	non-specific ST depression
low amplitude T-waves	ventricular premature complex
non-diagnostic T abnormalities	inverted T-waves
short PR interval	atrial premature complex
Rhythm	
sinus bradycardia	supraventricular tachycardia
sinus rhythm	sinus tachycardia
atrial bradycardia	atrial fibrillation
sinus arrhythmia	normal functioning artificial pacemaker
atrial flutter	trigeminal pattern
paroxysmal supraventricular tachycardia	bigeminal pattern
Miscellaneous	
burst noise	old stage of myocardial infarction
static noise	early stage of myocardial infarction
baseline drift	middle stage of myocardial infarction
electrodes problems	left axis deviation
ventricular extrasystoles	right axis deviation
supraventricular extrasystoles	

Table 8. Sample QA templates for tasks.

Questions	
Closed-QA	<p>1. Please assign the most suitable shape and structure classification with a detailed examination of the provided ECG sequence of this subject. A. Non-diagnostic T abnormalities; B. Ventricular premature complex; C. Low QRS voltage in limb leads; D. Non-specific ST elevation.</p> <hr/> <p>2. Investigate the patient's ECG reading and diagnose its classification based on its features. A. Normal ECG; B. Incomplete left bundle branch block; C. Long QTc-interval; D. Complete right bundle branch block.</p> <hr/> <p>3. By conducting a detailed evaluation of the ECG trace of the person, output the correct rate and regularity it should be classified under. A. Bigeminal pattern; B. Sinus tachycardia; C. Sinus rhythm; D. Normal functioning artificial pacemaker.</p> <hr/> <p>4. What would you determine the pattern and timing of this ECG reading to be? A. Atrial fibrillation; B. Atrial flutter; C. Normal functioning artificial pacemaker; D. No abnormality detected.</p> <hr/> <p>5. With precision and attention to detail, work through the subject's ECG reading and give the most appropriate rhythm based on its characteristics. A. Sinus bradycardia; B. Atrial flutter; C. Paroxysmal supraventricular tachycardia; D. Atrial fibrillation.</p>
Open-QA	<p>1. Given the ECG finding, please work through its features and classify the right shape and structure.</p> <hr/> <p>2. Assign the waveform associated with the ECG characteristic.</p> <hr/> <p>3. What pattern and timing does ECG interpretation exhibit?</p> <hr/> <p>4. Through meticulous examination of the patient's ECG sequence, please accurately determine the diagnosis that best defines it.</p> <hr/> <p>5. What rhythm does the given ECG characteristic from the patient exhibit?</p>
Comparison-QA	<p>1. Has non-diagnostic T abnormalities been eliminated in the recent tracing in comparison to the previous one?</p> <hr/> <p>2. Does the second ECG still indicate the presence of ST/T change as compared to the first ECG?</p> <hr/> <p>3. Is atrial flutter still not detected in the recent tracing when compared to the previous one?</p> <hr/> <p>4. Does the second ECG still show the absence of non-specific T-wave changes when compared to the first ECG?</p> <hr/> <p>5. Is the RR interval still considered normal in the latest tracing when compared to the previous tracing?</p>
Report Generation	<p>1. Please provide a comprehensive ECG interpretation for this 69.0-year-old male individual.</p> <hr/> <p>2. Produce a detailed ECG analysis for this 55.0-year-old female case.</p> <hr/> <p>3. Generate a standardized ECG assessment report for this 36.0-year-old male patient.</p> <hr/> <p>4. Based on the ECG signal from this 75.0-year-old male patient, generate a structured clinical 12-lead ECG report.</p> <hr/> <p>5. Analyze the ECG tracing and generate a clinical report for this 77.0-year-old male individual.</p>
Answers	
Positive Condition	<p>1. Based on the ECG pattern, after thorough examination, the form is classified as {condition}.</p> <hr/> <p>2. The diagnostic classification observed in the given ECG observation suggests a evident link to suggestive of {condition}.</p> <hr/> <p>3. After systematic analysis, the ECG evaluation is classified as {condition}.</p> <hr/> <p>4. Clinical findings from this ECG assessment reinforce the presence of {condition} as a evident outcome.</p> <hr/> <p>5. The ECG signal shows evidence of {condition}.</p>
Negative Condition	<p>1. All leads demonstrate physiological waveforms, and the overall conclusion is a normal ECG.</p> <hr/> <p>2. Standard diagnostic criteria confirm that the signal is entirely normal, with no pathological findings.</p> <hr/> <p>3. No evidence of ST-segment elevation, depression, or T-wave inversions.</p> <hr/> <p>4. Healthy cardiac activity.</p> <hr/> <p>5. Heart rate is regular, with consistent P-P and R-R intervals.</p>

Table 9. Evaluation dimensions and weighted criteria for ECG diagnostic reports.

Category	Evaluation Criteria	Weight
Diagnostic Completeness	Completeness of abnormal features mentioned	10
	Completeness of key diagnoses included	10
	Absence of critical diagnostic errors	10
	Whether the report describes severity or likelihood of the findings	8
	Whether the report includes suspected diagnoses	7
Form Accuracy	Correct identification of anatomical regions (e.g., P/QRS/T waves)	8
	Correct recognition of waveform abnormalities (e.g., ST elevation/depression)	7
Rhythm Accuracy	Correct classification of baseline rhythm (e.g., sinus or ectopic)	4
	Correct classification of arrhythmias (e.g., tachycardia or bradycardia)	4
	Correct interpretation of conduction abnormalities (e.g., location and degree of block)	4
	Accurate detection of pacing signals	3
Report Logic	Report is well-structured and logically organized	5
	Findings are explained in a point-wise or categorized manner	4
	Includes relevant auxiliary information (e.g., age, gender, etc.)	3
	Patient privacy is protected via anonymization	3
Descriptive Norms	Terminology complies with SCP-ECG standards (e.g., use “complete right bundle branch block” instead of “RBBB”)	5
	Language avoids inappropriate certainty (e.g., avoids overconfident conclusions)	5
Total Score		100

C. Supplemental Experimental Results

C.1. Ablation Study Results of HeartcareGPT

For completeness, we present in this appendix the full numerical results of all ablation settings of HeartcareGPT-3.8B discussed in Section 6.3. While the main paper visualizes the trends through figures, the detailed data tables are provided here to enable transparent comparison across all variants of the training pipeline (shown in Table 10, 11, 12 and 13) and multimodal integration strategies (shown in Table 14, 15, 16 and 17).

Across all settings, the ablation results consistently validate the effectiveness of our design choices. Removing either Beat training stage or warming up stage leads to substantial degradation in diagnostic accuracy and multimodal alignment. Likewise, replacing our tri-modal fusion with single-modality variants or removing 12-lead sub-image segmentation yields clear declines in performance. These trends reinforce the necessity of (i) ECG-aware representation modeling, (ii) stabilized multimodal projection, and (iii) fine-grained visual decomposition for enhancing clinical

reasoning.

Overall, the full quantitative data reported here further substantiate our claims: each architectural and training design contributes meaningfully to HeartcareGPT’s superior diagnostic capability and its robustness across diverse ECG modalities.

C.2. Ablation Study Results of Beat

To validate the performance of our model, we conduct comprehensive experiments based on our ECG tokenizer, Beat. We evaluate its capabilities in both signal reconstruction and prediction tasks under various structural configurations, including the use of dual-level vector quantization (DVQ) structure, codebook size, and input sequence length.

In Section 5.1, we have introduced the joint supervision strategy adopted in Beat. To facilitate evaluation in experiments, we also consider this total loss as a quantitative metric. Specifically, the overall training objective of Beat is defined as $\mathcal{L}_{\text{total}} = \lambda_1 \mathcal{L}_{\text{recon}} + \lambda_2 \mathcal{L}_{\text{pred}} + \lambda_3 \mathcal{L}_{\text{VQ}}$, where we set $\lambda_1 = 1.0$, $\lambda_2 = 0.5$ and $\lambda_3 = 0.25$ in our experiments, balancing the contributions of reconstruction, prediction, and

Evaluation Prompt

System Prompt:

You are a professional cardiac expert. The diagnostic accuracy of the generated report was judged according to the reference report. There are 17 evaluation indicators, and the calculation method and examples of each indicator are given below. Please compare the generated report with the reference report and score strictly according to the evaluation criteria.

Instruction:

- **Reference Report:** {REFERENCE_REPORT}
- **Generated Report:** {GENERATED_REPORT}
- **Evaluation Criteria:**
 1. Completeness of abnormal features mentioned (higher=more complete): **10**,
 2. Completeness of key diagnoses included (higher=more complete): **10**,
 3. Absence of critical diagnostic errors (higher=better): **8**,
 - ...
 17. Whether wording is appropriate, avoiding absolute expressions: **5**
- **Requirements:**
 1. Score each item in the criteria above from 0 to 100 based on comparison with the reference report.
 - A score **from 90 to 100** indicates full compliance with the description;
 - A score **from 80 to 89** indicates substantial compliance with the description;
 - A score **from 60 to 79** indicates partial non-compliance with certain aspects;
 - A score **below 60** indicates complete non-compliance.
 2. Calculate weighted dimension scores: $score_i \times weight_i$.
 3. The final total score is the sum of all weighted dimension scores:
 $total_score = \sum(score_i \times weight_i) / \sum(weight_i)$.
 4. The output must be in the form of JSON:

```
{
  "item_scores": {
    "1": score_1, "2": score_2, ..., "17": score_17
  },
  "total_score": total_score
}
```

Figure 8. Prompt for report evaluation.

Table 10. Ablation study on training stages for HeartcareGPT-3.8B on *closed-QA* tasks from our proposed Heartcare-Bench^S and Heartcare-Bench^I.

Training Beat	Warming up	Heartcare-Bench ^S				Heartcare-Bench ^I				Avg.
		Diagnosis	Waveform	Rhythm	Misc.	Diagnosis	Waveform	Rhythm	Misc.	
-	-	37.70	53.06	45.71	63.22	43.17	49.64	40.41	34.54	45.93
-	☑	45.82	64.37	57.28	<u>72.25</u>	51.86	60.91	50.19	44.69	55.92
☑	-	<u>74.13</u>	<u>87.10</u>	<u>75.86</u>	71.90	<u>82.03</u>	<u>83.74</u>	<u>71.62</u>	<u>65.38</u>	<u>76.47</u>
☑	☑	81.95	95.94	82.79	79.84	87.85	92.21	79.25	67.80	83.33

vector-quantization objectives. By monitoring the overall training objective as well as its individual components, we can more thoroughly assess how each architectural modifica-

tion affects representation quality and optimization stability.

For a more comprehensive evaluation of Beat’s performance, we additionally employ the codebook utilization as

Table 11. Ablation study on training stages for HeartcareGPT-3.8B on *open-QA* tasks from our proposed Heartcare-Bench^S and Heartcare-Bench^I.

Training Beat	Warming up	Heartcare-Bench ^S								Heartcare-Bench ^I							
		Diagnosis		Waveform		Rhythm		Misc.		Diagnosis		Waveform		Rhythm		Misc.	
		F1-Bio	Rouge-L	F1-Bio	Rouge-L	F1-Bio	Rouge-L	F1-Bio	Rouge-L	F1-Bio	Rouge-L	F1-Bio	Rouge-L	F1-Bio	Rouge-L	F1-Bio	Rouge-L
-	-	50.32	23.15	57.84	28.97	49.35	25.42	60.27	24.32	53.81	27.19	55.04	25.96	50.91	25.30	56.67	26.18
-	✓	61.18	<u>31.84</u>	61.23	36.95	66.59	<u>33.98</u>	58.72	<u>30.21</u>	52.84	28.12	53.47	<u>32.87</u>	61.12	<u>32.45</u>	55.78	31.55
✓	-	<u>66.84</u>	28.21	<u>69.42</u>	32.89	<u>75.23</u>	33.12	<u>63.45</u>	28.34	<u>60.71</u>	31.59	<u>69.12</u>	29.75	<u>73.67</u>	31.34	64.27	28.09
✓	✓	68.53	32.27	72.74	<u>35.38</u>	78.63	36.42	65.84	30.97	63.17	<u>29.83</u>	70.92	33.57	75.36	34.69	<u>61.53</u>	<u>28.24</u>

Table 12. Ablation study on training stages for HeartcareGPT-3.8B on *comparison-QA* tasks from our proposed Heartcare-Bench^C.

Training Beat	Warming up	S-S		I-I		S-I		Avg.
		Cons.	Irr.	Cons.	Irr.	Cons.	Irr.	
-	-	44.61	45.18	47.52	51.44	49.68	52.12	48.43
-	✓	48.55	50.22	53.18	55.01	48.87	51.23	51.18
✓	-	<u>63.77</u>	70.44	<u>68.45</u>	<u>69.38</u>	<u>72.14</u>	<u>77.29</u>	<u>70.25</u>
✓	✓	66.40	<u>67.47</u>	69.88	75.19	78.71	78.83	72.74

Code%, which quantifies the proportion of codebook entries actually used during encoding.

As shown in Table 18, the results show that the DVQ structure with a codebook size of 512 and an input length of 1000 strikes a favorable balance between compression efficiency and semantic completeness. Notably, while smaller codebooks or shorter input sequences can achieve higher codebook utilization, their overall loss is higher than our chosen configuration, highlighting that code utilization alone is not sufficient to evaluate tokenizer effectiveness.

We summarize the following observations: (i) The DVQ structure captures global rhythm patterns via the core codebook and refines local variations via the residual codebook, thereby enhancing the clinical semantic integrity of the discrete representation while maintaining a compact token space. (ii) Enlarging the codebook increases representational granularity but leads to codebook collapse and lower utilization, whereas a smaller codebook fails to capture the complex pathological semantics of ECG signals. (iii) Excessively long or short input sequences degrade codebook utilization and introduce instability in reconstruction and prediction, likely due to imbalanced temporal context or fragmented signal structure. Overall, Beat achieves an effective global-local modeling trade-off through structural and parametric design, significantly improving the quality of ECG tokenization and enabling end-to-end training of ECG and text modalities within Med-MLLMs.

Furthermore, Figure 9 provides a comprehensive visualization of Beat’s reconstruction and prediction performance, demonstrating the model’s capability to accurately recover input patterns while generating high-fidelity future predictions.

D. Case Study

In this section, we compare generated answers of our proposed HeartcareGPT-3.8B with those of a generalist model (Claude-3.5) and a medical model (MedVLM-R1-2B). Since closed-QA and comparison-QA primarily contain selection-based questions, which are less illustrative for qualitative comparison, we focus on open-QA and report generation cases where the model’s reasoning, language, and clinical documentation capabilities can be more clearly observed. Figures 10 and 11 illustrate the performance of these three models on open-QA and report generation tasks. We highlight statements that match the ground truth in green, and indicate discrepancies with red.

As shown in Figure 10, HeartcareGPT’s response closely matches the reference answer, showing its precise understanding of detailed diagnostic questions.

A similar observation can be made from Figure 11. HeartcareGPT produces reports that not only capture clinically relevant findings with high accuracy, but also maintain clear structure. Moreover, the reports shows correct usage of ECG-specific phrasing and logical flow.

E. Limitations

Heartcare Suite advances multimodal ECG understanding with potential benefits for clinical diagnosis, medical AI research, and patient care. By integrating raw ECG signals and structured reports, it enables accurate, automated cardiac analysis, particularly valuable in resource-limited settings. The release of Heartcare-400K (the first large-scale ECG instruction dataset) and Heartcare-Bench (a standardized evaluation framework) fosters transparency and progress in medical AI. However, limitations include dataset biases (e.g.,

Table 13. Ablation study on training stages for HeartcareGPT-3.8B on *report generation* tasks from our proposed Heartcare-Bench^S and Heartcare-Bench^I.

Training Beat	Warming up	Heartcare-Bench ^S			Heartcare-Bench ^I		
		Score ^{GPT}	F1-Rad	Rouge-L	Score ^{GPT}	F1-Rad	Rouge-L
-	-	55.12	17.11	26.05	60.32	19.57	30.27
-	✔	65.21	20.11	29.64	<u>68.02</u>	21.14	30.89
✔	-	<u>64.33</u>	<u>22.12</u>	<u>32.20</u>	66.29	<u>22.78</u>	<u>35.43</u>
✔	✔	61.29	26.84	34.39	78.50	23.10	38.68

Table 14. Ablation study on multimodal integration for HeartcareGPT-3.8B on *closed-QA* tasks from our proposed Heartcare-Bench^S and Heartcare-Bench^I. Seg. = Image segmentation.

Signal	Image	Seg.	Heartcare-Bench ^S				Heartcare-Bench ^I				Avg.
			Diagnosis	Waveform	Rhythm	Misc.	Diagnosis	Waveform	Rhythm	Misc.	
•	✔	✔	74.83	87.12	76.46	73.42	80.91	88.05	69.43	53.36	75.45
✔	-	-	72.61	85.37	74.84	63.92	75.46	86.19	71.43	56.18	73.25
✔	✔	-	<u>79.12</u>	<u>93.26</u>	<u>81.64</u>	<u>76.43</u>	<u>84.98</u>	<u>87.65</u>	<u>77.43</u>	<u>62.84</u>	<u>80.42</u>
✔	✔	✔	81.95	95.94	82.79	79.84	87.85	92.21	79.25	67.80	83.33

underrepresentation of rare conditions), potential signal fidelity loss in tokenization, and untested real-time monitoring capabilities. Computational costs and regulatory hurdles for clinical deployment remain challenges. Future work should expand data diversity, optimize real-time processing, and validate clinical utility through trials.

Table 15. Ablation study on multimodal integration for HeartcareGPT-3.8B on *open-QA* tasks from our proposed Heartcare-Bench^S and Heartcare-Bench^I.

Signal	Image	Seg.	Heartcare-Bench ^S								Heartcare-Bench ^I							
			Diagnosis		Waveform		Rhythm		Misc.		Diagnosis		Waveform		Rhythm		Misc.	
			F1-Bio	Rouge-L	F1-Bio	Rouge-L	F1-Bio	Rouge-L	F1-Bio	Rouge-L	F1-Bio	Rouge-L	F1-Bio	Rouge-L	F1-Bio	Rouge-L	F1-Bio	Rouge-L
-	✓	✓	36.26	19.91	59.33	31.04	62.47	29.30	49.72	24.16	55.39	25.47	58.84	27.69	59.65	28.94	47.42	22.92
✓	-	-	38.74	21.56	51.62	26.83	64.29	<u>30.84</u>	36.67	23.05	43.68	22.19	48.56	24.71	50.97	25.64	32.12	20.14
✓	✓	-	<u>58.18</u>	<u>29.47</u>	<u>70.79</u>	<u>33.56</u>	<u>75.91</u>	29.28	<u>63.87</u>	<u>30.29</u>	<u>62.43</u>	29.96	<u>69.71</u>	<u>32.65</u>	<u>73.48</u>	<u>32.61</u>	<u>60.28</u>	31.34
✓	✓	✓	68.53	32.27	72.74	35.38	78.63	36.42	65.84	30.97	63.17	<u>29.83</u>	70.92	33.57	75.36	34.69	61.53	<u>28.24</u>

Table 16. Ablation study on multimodal integration for HeartcareGPT-3.8B on *comparison-QA* tasks from our proposed Heartcare-Bench^C.

Signal	Image	Seg.	S-S		I-I		S-I		Avg.
			Cons.	Irr.	Cons.	Irr.	Cons.	Irr.	
			-	✓	✓	48.23	57.79	56.91	
✓	-	-	51.46	61.32	53.65	52.83	64.25	67.01	58.42
✓	✓	-	<u>59.64</u>	<u>63.72</u>	<u>62.58</u>	<u>65.84</u>	<u>67.61</u>	<u>71.51</u>	<u>65.15</u>
✓	✓	✓	66.40	67.47	69.88	75.19	78.71	78.83	72.74

Table 17. Ablation study on multimodal integration for HeartcareGPT-3.8B on *report generation* tasks from our proposed Heartcare-Bench^S and Heartcare-Bench^I.

Signal	Image	Seg.	Heartcare-Bench ^S			Heartcare-Bench ^I		
			Score ^{GPT}	F1-Rad	Rouge-L	Score ^{GPT}	F1-Rad	Rouge-L
			-	✓	✓	58.46	16.83	33.29
✓	-	-	<u>61.92</u>	19.34	30.18	67.74	<u>21.99</u>	32.32
✓	✓	-	64.37	<u>23.76</u>	<u>33.84</u>	<u>70.13</u>	21.84	<u>34.49</u>
✓	✓	✓	61.29	26.84	34.39	78.50	23.10	38.68

Table 18. Ablation study for Beat under different configurations.

DVQ Structure	Codebook Size	Input Length	Code%	\mathcal{L}_{total}
-	512	1000	93.75	1.00
✓	1024	1000	79.50	<u>0.79</u>
✓	256	1000	99.87	0.81
✓	512	1500	91.46	1.10
✓	512	500	<u>98.20</u>	0.83
✓	512	1000	96.22	0.76

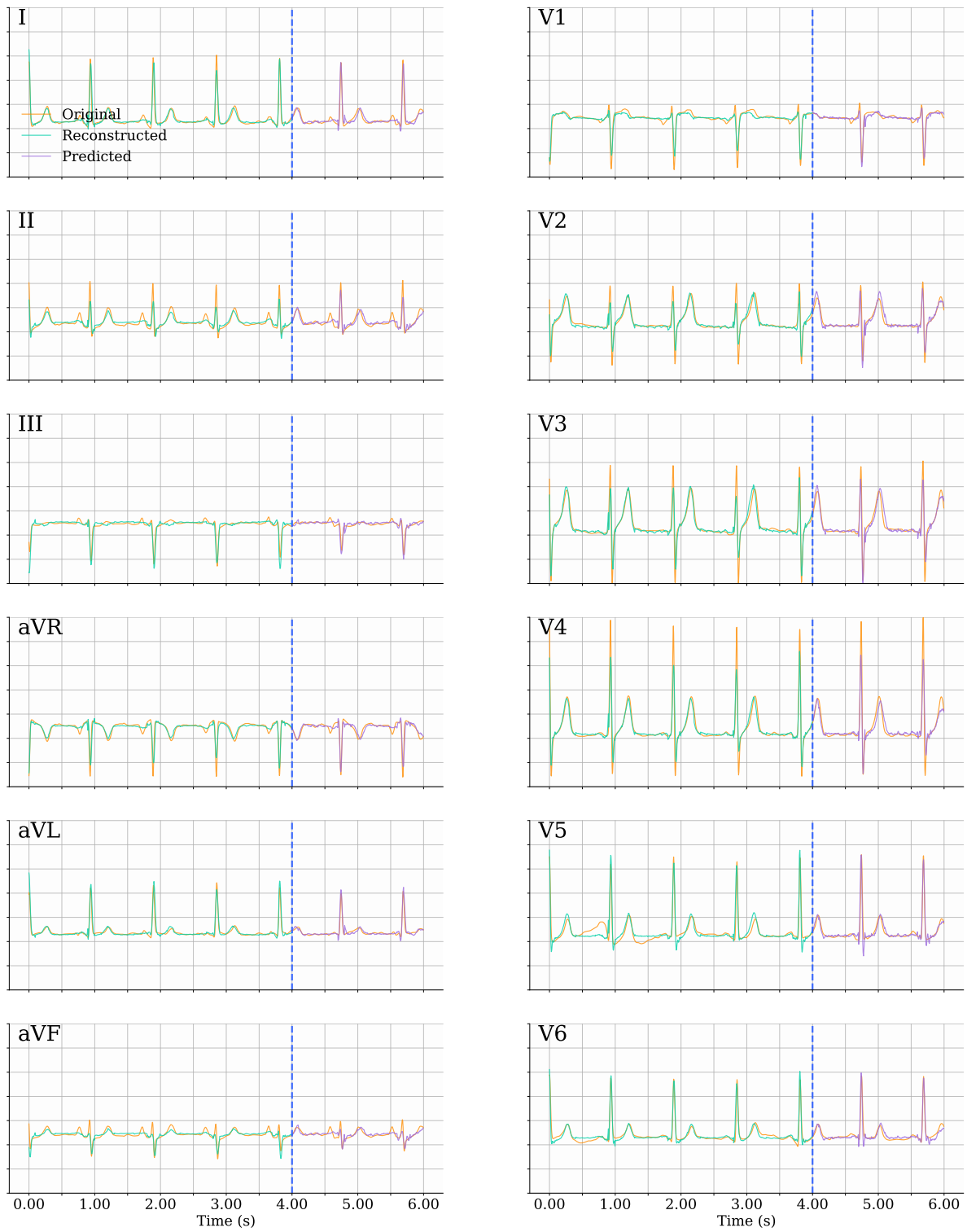


Figure 9. ECG signal reconstruction and prediction with Beat.

Question

Considering the ECG results of a 67-year-old female patient, what is the primary diagnosis?

Ground Truth

Anteroseptal myocardial infarction

HeartcareGPT

Ventricular premature complex and myocardial infarction.

MedVLM-R1-2B

The primary diagnosis for this patient is a 12-lead ECG showing ST-segment elevation in the inferior wall of the heart.

Claude-3.5

The ECG indicates Atrial Fibrillation with a rapid ventricular response.

Figure 10. A case of *open-QA* tasks.

Question

Please provide a comprehensive ECG interpretation for this 69.0-year-old male individual.



Ground Truth

First Degree AV Block

HeartcareGPT

Clinical 12-lead ECG Report

Patient Information:

- Age: 69 years
- Gender: Male

ECG Findings:

Diagnosis:

- **First Degree AV Block:** Highly likely (100.0% probability)
- Non-specific Ischemic Changes: Less likely (15.0% probability)

Rhythm:

- Baseline rhythm: Normal sinus rhythm
- Conduction issues: Presence of first degree AV block

Waveform:

- No significant waveform abnormalities detected

Summary:

This ECG indicates a **first degree AV block**, consistent with delayed AV node conduction. There is a low likelihood of non-specific ischemic changes. Overall, the minor conduction anomaly observed does not suggest severe cardiac pathology at present.

MedVLM-R1-2B

The ECG of this 69.0-year-old male individual shows a sinus rhythm with a **right bundle branch block (RBBB) pattern**. The rhythm is regular, and the waveform is normal. The RBBB pattern indicates that the electrical signals in the right bundle branch are delayed or blocked, which can affect the heart's ability to pump blood effectively. However, the overall ECG findings are **normal**, suggesting that the patient's heart function is within the expected range for his age.

Claude-3.5

ECG Report

Rhythm Description:

- Regular sinus rhythm
- Heart rate approximately 75-80 beats per minute
- Consistent P-QRS-T wave morphology across all leads

Key Waveform Findings:

- Normal P wave morphology and axis
- QRS complexes: Normal duration (0.08-0.10 seconds)
- ST segments: Isoelectric
- T waves: Upright and symmetrical in most leads
- No significant Q waves
- No ST segment elevation or depression
- No evidence of acute ischemia or infarction

Interpretation/Summary:

Normal 12-lead ECG demonstrating a stable sinus rhythm with **no significant pathological findings**. The electrical conduction system appears intact, with normal wave morphology and intervals. No acute cardiac abnormalities are detected in this tracing for this 69-year-old male patient.

Recommendations:

- **Routine clinical correlation**
- **No urgent cardiac interventions** suggested based on this ECG

Figure 11. A case of report generation tasks.